JOC Article

Circular Dichroism of Intra- and Intermolecular Charge-Transfer Complexes. Enhancement of Anisotropy Factors by Dimer Formation and by Confinement

Tadashi Mori,*[,†,‡] Young Ho Ko,[§] Kimoon Kim,[§] and Yoshihisa Inoue*[,†,∥]

Department of Molecular Chemistry, Graduate School of Engineering, Osaka University, 2-1 Yamada-oka, Suita 565-0871, Japan, Theoretische Organische Chemie, Organish-Chemisches Institut der Universität Münster, Corrensstraaβe 40, D-48149 Münster, Germany, National Creative Research Initiative Center for Smart Supramolecules and Department of Chemistry, Division of Molecular and Life Sciences, Pohang University of Science and Technology, San 31 Hyojadong, Pohang 790-784, Republic of Korea, and the Entropy Control Project, ICORP, JST, 4-6-3 Kamishinden, Toyonaka 560-0085, Japan

tmori@chem.eng.osaka-u.ac.jp; inoue@chem.eng.osaka-u.ac.jp

Received February 8, 2006

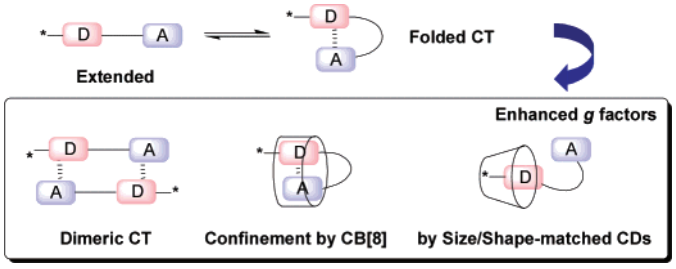

The dynamic behavior of new CT-dyads (CT = charge transfer) has been studied by means of UV−vis, fluorescence, and NMR spectroscopies under a variety of conditions. It was found that the CT-dyads exhibit conformational variations, such as extended and folded monomers and an antiparallel dimer complex, depending on the conditions. The CT interaction was found in the folded conformation at ambient temperature, while the contribution of the dimeric species became evident at lower temperatures. Most interestingly, close examinations of the circular dichroism spectra of these CT-dyads reveal that the anisotropy (*g*) factors of the dimers are significantly enhanced by a factor of ∼30 in the CT transition region. Such enhancement is rationalized in terms of the stronger CT interactions in the dimer through the double electronic coupling element, which imposes stronger restrictions on the rotation of alkyl group(s). Confinement of the CT-dyads in cyclodextrin (CD) and cucurbituril cavities afforded further insights into the chiroptical properties of the CT-dyad. The effects of confinement are clearly size-dependent, exhibiting a substantial enhancement of the *g* factors by a factor of 5−10 upon inclusion by *β*-CD and also by cucurbit[8]uril, but with no appreciable changes upon complexation with the other CDs. These results indicate that the conformational fixation of CT-dyads, for example by dimer formation or by confinement in size/shape-matched cavities, is a conventional, yet powerful, tool for manipulating (mostly enhancing) the chiroptical properties of the CT transition, which should be applicable in general to a variety of molecular and supramolecular CT systems.

Introduction

Recently, charge-transfer (CT) interactions[1,2] between aromatic donors and acceptors have been greatly exploited in developing molecular and supramolecular assemblies such as rotaxanes and catenanes[3] and molecular sensing and electronic devices such as sensors and switches, as well as nonlinear optical materials.[4] However, there are only a limited number of systems that have successfully afforded stable intramolecular CT complexes.[5,6] Recently, host-induced CT complexation with cucurbit[8]uril (CB[8]) has been employed for efficiently constructing complex molecular assemblies, such as pentameric molecular

* To whom correspondence should be addressed. Fax: +81-6-6879-7923. Tel.: +81--6879-7920.
† Osaka University.
‡ Universität Münster.
§ Pohang University of Science and Technology.
∥ ICORP, JST.

10.1021/jo0602672 CCC: $33.50
Published on Web 03/16/2006

necklaces and large vesicles.[7] Weak ground-state interactions, including CT, should be significantly affected by environmental factors such as solvent polarity, temperature, and pressure. These entropy-related factors are known to influence photochemical and photophysical behavior and have been exploited for controlling asymmetric photoreactions.[8] We have also demonstrated that the diastereoselectivity of the [2+2] photocycloaddition of *trans*-stilbene to chiral alkyl fumarate is greatly affected by solvent polarity, temperature, and pressure upon CT and/or direct excitation.[9]

Electronic circular dichroism (ECD) spectroscopy is an essential and powerful tool for obtaining the chiroptical and stereochemical information of optically active molecules in solution. Ample examples of the ECD spectra of various organic and bioorganic compounds have been recently accumulated.[10] Nevertheless, practically no systematic attempts have hitherto been devoted to the ECD spectral study of CT transitions.[11,12]

SCHEME 1

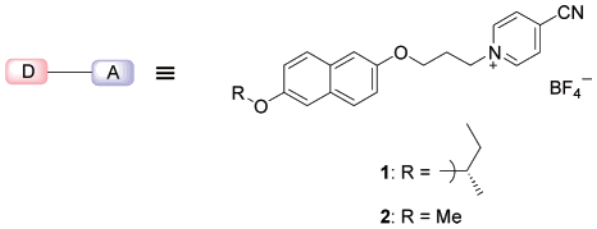

In the present study, we report the ECD spectra of the chirally modified intramolecular CT complex (CT-dyad **1**) under a variety of conditions. We will focus particularly on how the *g* factor of a CT transition is affected through the structural changes of the CT-dyad caused by altering the solvent, concentration, and temperature and also by confining the molecule in nanospace. The structure and dynamic behavior of the CT-dyad in the ground and excited states under the given conditions will be first assessed by UV−vis, fluorescence, and NMR spectroscopies, and then the relationship between the structure and the chiroptical properties of CT-dyad will be elucidated by combining these data with those from the circular dichroism spectral examinations.

Results and Discussion

In our initial attempt to elucidate how and to what extent the *g* factor can be modified by CT interactions, we designed a novel tethered donor−acceptor system, that is, CT-dyads **1** (R = (*S*)-1-methylpropyloxy) and **2** (R = Me), shown in Scheme 1. Possessing a sufficiently low oxidation potential of 1.1−1.3 V (versus SCE),[13] the 2,6-dialkoxynaphthalene unit is expected to function as a good donor. Compared to rigid linker systems using steroid, norbornane, and peptide spacers,[14] our flexible linker system with a polymethylene chain gives the system more freedom to finely tune its conformation and optimize donor−acceptor interactions. It is well-documented that the trimethylene linker is most efficient for intramolecular electronic interactions.[15] As an acceptor, we chose the 4-cyanopyridinium cation, which is expected to act as an electron acceptor ($E_{1/2}^{red} = -0.64$ V versus SCE),[16] forming an intramolecular CT complex with the dialkoxynaphthalene unit in the dyad.[16,17] Because the counteranion of the pyridinium salt, particularly iodide, may act as an electron donor to form a CT complex within the salt,[17]

(1) For recent reviews, see: (a) Frenking, G.; Wichmann, K.; Frohlich, N.; Loschen, C.; Lein, M.; Frunzke, J.; Rayon, V. M. *Coord. Chem. Rev.* **2003**, *238*−*239*, 55−82. (b) Arnold, B.; Levy, D.; McKirr, W. *Spectrum* **2003**, *16*, *8*−*11*, 17. (c) Rosokha, S. V.; Kochi, J. K. *J. Org. Chem.* **2002**, *67*, 1727−1737. (d) Yan, Y. J.; Zhang, H. J. *Theor. Comput. Chem.* **2002**, *1*, 225−244. (e) Rosokha, S. V.; Kochi, J. K. *Mod. Arene Chem.* **2002**, 435−478. (f) Hunter, C. A.; Lawson, K. R.; Perkins, J.; Urch, C. J. *J. Chem. Soc., Perkin Trans. 2* **2001**, 651−669. (g) Hubig, S. M.; Lindeman, S. V.; Kochi, J. K. *Coord. Chem. Rev.* **2000**, *200*−*202*, 831−873.

(2) (a) Foster, A. *Organic Charge-Transfer Complexes*; Academic Press: New York, 1969. (b) Mulliken, R. S.; Person, W. B. *Molecular Complexes*; Wiley: New York, 1969. (c) Foster, R. *Molecular Complexes*; Crane, Russak & Co.: New York, 1974; Vol. 2.

(3) For reviews on molecular assembly, see: (a) Philip, D.; Stoddart, J. F. *Angew. Chem., Int. Ed. Engl.* **1996**, *35*, 1154−1196. (b) Amabilino, D. B.; Stoddart, J. F. *Chem. Rev.* **1995**, *95*, 2725−2828.

(4) For reviews on molecular materials based on donor−acceptor interactions, see: (a) Nielsen, M. B.; Lomholt, C.; Becher, J. *Chem. Soc. Rev.* **2000**, *29*, 153−164. (b) Bryce, M. R. *Adv. Mater.* **1999**, *11*, 11−23.

(5) (a) Nielsen, M. B.; Nielsen, S. B.; Becher, J. *Chem. Commun.* **1998**, 475−476. (b) Ashton, P. R. et al. *Chem.—Eur. J.* **1997**, *3*, 152−170 (for complete reference, see Supporting Information).

(6) Park, J. W.; Lee, B. A.; Lee, S. Y. *J. Phys. Chem. B* **1998**, *102*, 8209−8215.

(7) (a) Kim, H.-J.; Heo, J.; Jeon, W. S.; Lee, E.; Kim, J.; Sakamoto, S.; Yamaguchi, K.; Kim, K. *Angew. Chem., Int. Ed.* **2001**, *40*, 1526−1529. (b) Lee, J. W.; Kim, K.; Choi, S. W.; Ko, Y. H.; Sakamoto, S.; Yamaguchi, K.; Kim, K. *Chem. Commun.* **2002**, 2692−2693. (c) Ko, Y. H.; Kim, K.; Kang, J.-K.; Chun, H.; Lee, J. W.; Sakamoto, S.; Yamaguchi, K.; Fettinger, J. C.; Kim, K. *J. Am. Chem. Soc.* **2004**, *126*, 1932−1933. (d) Jeon, W. S.; Kim, E.; Ko, Y. H.; Hwang, I.; Lee, J. W.; Kim, S.-Y.; Kim, H.-J.; Kim, K. *Angew. Chem., Int. Ed.* **2005**, *44*, 87−91. (e) Jeon, Y. J.; Bharadwaj, P. K.; Choi, S. W.; Lee, J. W.; Kim, K. *Angew. Chem., Int. Ed.* **2002**, *41*, 4474−4476.

(8) (a) Inoue, Y.; Wada, T.; Asaoka, S.; Sato, H.; Pete, J.-P. *Chem. Commun.* **2000**, 251−259. (b) Nishiyama, Y.; Kaneda, M.; Saito, R.; Mori, T.; Wada, T.; Inoue, Y. *J. Am. Chem. Soc.* **2004**, *126*, 6568−6569. (c) Asaoka, S.; Wada, T.; Inoue, Y. *J. Am. Chem. Soc.* **2003**, *125*, 3008−3027. (d) Inoue, Y.; Ikeda, H.; Kaneda, M.; Sumimura, T.; Everitt, S. R. L.; Wada, T. *J. Am. Chem. Soc.* **2000**, *122*, 406−407.

(9) (a) Saito, H.; Mori, T.; Wada, T.; Inoue, Y. *J. Am. Chem. Soc.* **2004**, *126*, 1900−1906. (b) Saito, H.; Mori, T.; Wada, T.; Inoue, Y. *Chem. Commun.* **2004**, 1652−1653.

(10) (a) Berova, N.; Nakanishi, K.; Woody, R. W. *Circular Dichroism, Principles and Applications*, 2nd ed.; John Wiley & Sons: New York, 2000. (b) Lightner, D. A.; Gurst, J. E. *Organic Conformational Analysis and Stereochemistry from Circular Dichroism Spectroscopy*; John Wiley & Sons: New York, 2000.

(11) There have been several brief reports that describe the ORD and circular dichroism spectra of chiral CT complexes. (a) Briegleb, G.; Kuballe, H. G. *Angew. Chem.* **1964**, *76*, 228−229; *Angew. Chem., Int. Ed. Engl.* **1964**, *3*, 307−308. (b) Briegleb, G.; Kuball, H. G.; Henschel, K. *J. Phys. Chem. (Frankfurt)* **1965**, *46*, 229−249. (c) Briegleb, G.; Kuball, H. G.; Henschel, K.; Euing, W. *Ber. Bunsen-Ges. Phys. Chem.* **1972**, *76*, 101−105. (d) Geissler, U.; Schulz, R. C. *Makromol. Chem., Rapid Commun.* **1981**, *2*, 591−594. See also: (e) Wynberg, H.; Lammertsma, K. *J. Am. Chem.* Soc. **1973**, *95*, 7913−7914.

(12) For a preliminary communication, see: Mori, T.; Inoue, Y. *Angew. Chem., Int. Ed.* **2005**, *44*, 2582−2585.

(13) (a) Sato, C.; Kikuchi, K.; Okamura, K.; Takahashi, Y.; Miyashi, T. *J. Phys. Chem.* **1995**, *99*, 16925−16931. (b) Zweig, A.; Maurer, A. H.; Robert, B. G. *J. Org. Chem.* **1967**, *32*, 1322−1329.

(14) (a) Closs, G. L.; Miller, J. R. *Science* **1988**, *240*, 440−447. (b) Warman, J. M.; Smit, K. J.; de Haas, M. P.; Jonker, S. A.; Paddon-Row, M. N.; Oliver, A. M.; Kroon, J.; Oevering, H.; Verhoeven, J. W. *J. Phys. Chem.* **1991**, *95*, 1979−1987. (c) Jones, G.; Lu, L. N.; Fu, H.; Farahat, C. W.; Oh, C.; Greenfield, S. R.; Gosztola, D. J.; Wasielewski, M. R. *J. Phys. Chem. B* **1999**, *103*, 572−581.

(15) (a) Le, T. P.; Rogers, J. E.; Kelly, L. A. *J. Phys. Chem. A* **2000**, *104*, 6778−6785. (b) Siemiarczuk, A.; McIntosh, A. R.; Ho, T. F.; Stillman, M. J.; Roach, K. J.; Weedon, A. C.; Bolton, J. R.; Connolly, J. S. *J. Am. Chem. Soc.* **1983**, *105*, 7224−7230. (c) Chandross, E. A.; Dempster, C. J. *J. Am. Chem. Soc.* **1970**, *92*, 3586−3593. (d) Itoh, M. *J. Am. Chem. Soc.* **1972**, *94*, 1034−1035.

(16) Lee, K. Y.; Kochi, J. K. *J. Chem. Soc., Perkin Trans. 2* **1992**, 1011−1017.

(17) (a)Verhoeven, J. W.; Dirkx, I. P.; de Boer, T. J. *Tetrahedron* **1969**, *25*, 3395−3405. (b) Murthy, A. S. N.; Bhardwaj, A. P. *Spectrochim. Acta* **1983**, *39A*, 939−942.

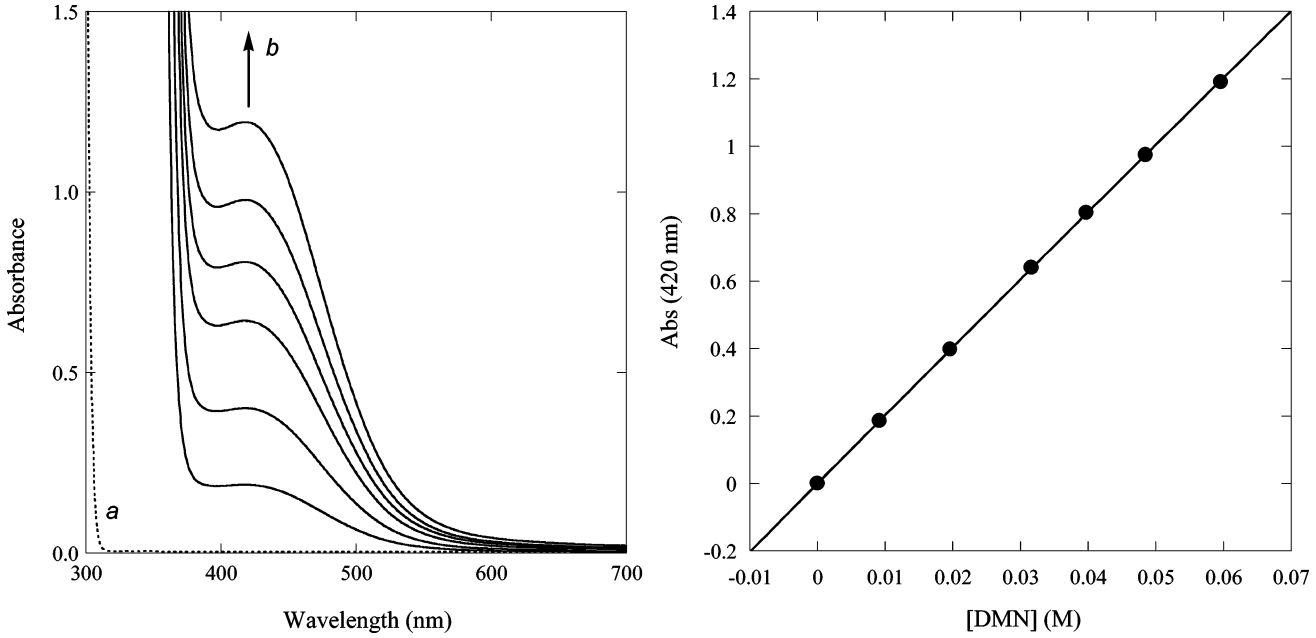

FIGURE 1. Left: UV−vis spectral changes of an acetonitrile solution of *N*-methyl-4-cyanopyridinium tetrafluoroborate (0.1 M) upon the incremental addition of 2,6-dimethoxynaphthalene at 25 °C. (a) *N*-Methyl-4-cyanopyridinium tetrafluoroborate only and (b) in the presence of 10, 20, 30, 40, 50, and 60 mM (from bottom to top) of 2,6-dimethoxynaphthalene; the CT absorption grew in intensity at 420 nm. Right: the concentration dependence of the CT absorption. The quasi-linear line represents the nonlinear least-squares fitting curve, assuming the 1:1 stoichiometry.

counteranions were exchanged to the less-coordinating and optically transparent tetrafluoroborates.[18]

Intermolecular Charge-Transfer Complexation of the Individual Donor and Acceptor. Before examining the CT-dyads **1** and **2**, we first investigated the intermolecular CT complexation behavior of the individual donor and acceptor units. Thus, the CT complexation of 2,6-dimethoxynaphthalene with *N*-methyl-4-cyanopyridinium was quantitatively investigated in acetonitrile at 25 °C by UV−vis spectroscopy. Upon the gradual addition of 2,6-dimethoxynaphthalene to a solution of *N*-methyl-4-cyanopyridinium at a fixed concentration, a new absorption, assignable to a CT complex, emerged at wavelengths 370−600 nm (Figure 1). The association constant (K_{CT}) was determined from the absorbance changes at the peak (420 nm) by a nonlinear least-squares fit to the following equation:

$$A_{420} = \frac{\epsilon_{CT}}{2}\sqrt{\left(C_D + C_A + \frac{1}{K_{CT}}\right) - \left(C_D + C_A + \frac{1}{K_{CT}}\right)^2 - 4C_DC_A}$$

The obtained association constant and molar extinction coefficient of the CT complex, $K_{CT} = 0.48 \pm 0.09$ M^{-1} and $\epsilon_{CT} = 445 \pm 75$ M^{-1} cm^{-1} ($\epsilon_{CT}K_{CT} = 214$), are comparable to those reported for a CT complex between 1,4-dimethylnaphthalene and *N*-methyl-4-cyanopyridinium ($\lambda_{max} = 410$ nm, $K_{CT} = 0.33$ M^{-1}, and $\epsilon_{CT} = 680$ M^{-1} cm^{-1}).[16]

Absorption and Fluorescence Spectral Examinations of the Intramolecular CT Complexation of 1. The UV−vis spectra of CT-dyads **1** and **2** are basically composed of two major transitions, displaying λ_{max}/nm (log ϵ) 232 (5.01), 261 (3.98), 269 (4.04), 285 (3.78, sh), 333 (3.43), and 345 (3.46; see Figure S1 in Supporting Information). However, a careful examination of the spectra revealed a weak broad absorption at about 420 nm as a shoulder, which is assignable to an inter- or intramolecular CT transition. As a typical example, the UV−vis spectra of **1** (3 mM) in acetonitrile, placed in cells of different light path lengths, are shown in the left panel of Figure 2. The small temperature dependence observed for this CT absorption (Figure S1, right) indicates the intramolecular nature of this band as well as the small entropy change involved upon (intramolecular) CT interaction (Figure S2). The good liner correlation found for the concentration dependence of absorption changes in acetonitrile and in dichloromethane (Figure 2, right) unequivocally demonstrated that the band is attributable to the *intra*molecular CT complex, at least up to the concentrations employed, that is, 10 mM in acetonitrile and 5 mM in dichloromethane (unfortunately, the low solubility of **1** did not allow us to examine at higher concentrations). Because it was shown that the π-ring systems of the CT complex are arranged cofacially to give a face-to-face interaction between 2,6-dimethoxynaphthalene and the viologen acceptor,[19] a folding of the polymethylene linkage is required for such an interaction in the linked compound **1** or **2**. Therefore, the folded conformation **A** is assumed to be in equilibrium with the more favored extended form **B** (Chart 1). The equilibrium constant for the intramolecular complexation (K_{int}), defined as a ratio of the folded conformer to the extended conformer, was evaluated as 0.25 in dichloromethane or 0.17 in acetonitrile, if we assume the same ϵ_{CT} for the folded conformer **A** and the value for an intermolecular CT complex between 2,6-dimethoxynaphthalene and *N*-methyl-4-cyanopyridinium tetrafluoroborate. A slightly larger K_{int} value in dichloromethane is probably due to the stronger CT interaction that favors delocalization of the positive charge of pyridinium in the less-polar solvent. Note that similar phenomena were also observed for the achiral analogue **2**, but less clearly seen as a result of the lower solubility of **2** in both solvents.

Temperature Dependence of the Fluorescence Spectra of

(18) Reed, C. A. *Acc. Chem. Res.* **1998**, *31*, 133−139.

(19) Yoon, K. B.; Kochi, J. K. *J. Phys. Chem.* **1991**, *95*, 3780−3790.

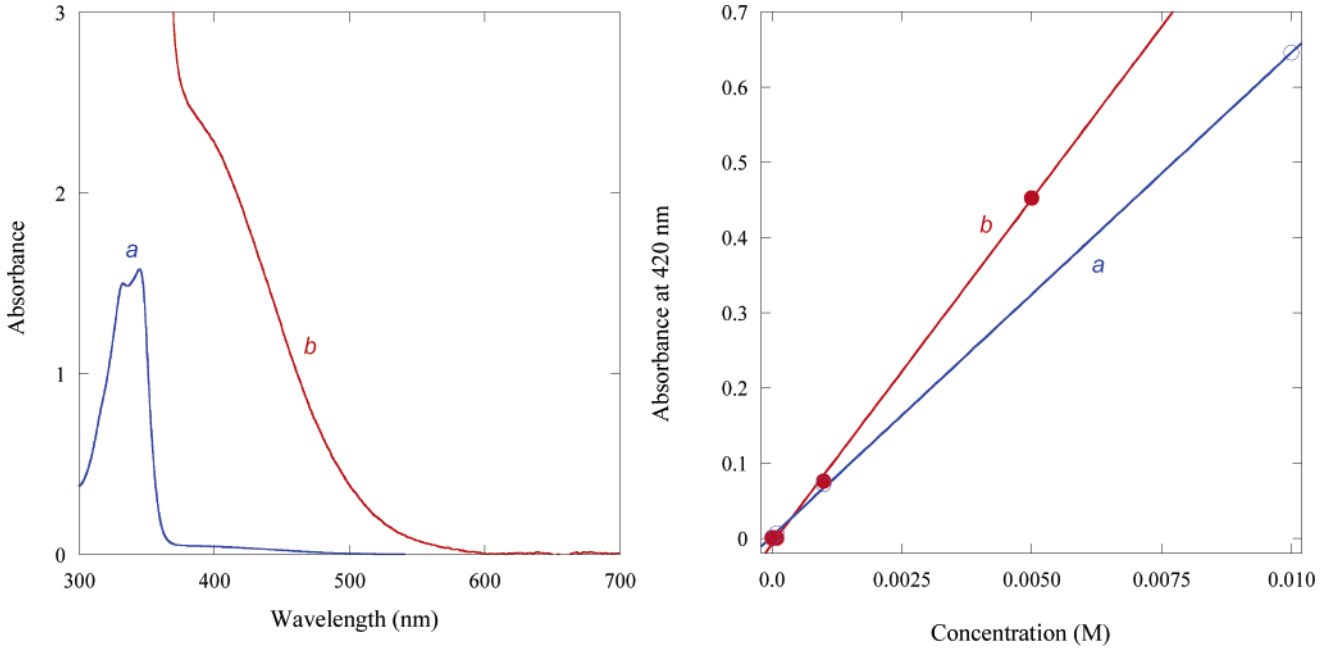

FIGURE 2. Left: absorption spectra of an acetonitrile solution of **1** (3 mM) at 25 °C placed in a cell of a (a) 0.2-cm or (b) 10-cm light path. Right: the increase in absorbance at 420 nm (CT complex) as a function of the concentration of **1** in (a) acetonitrile or (b) dichloromethane at 25 °C. Regression lines: $A_{CH_2Cl_2} = 89.9 \times [\mathbf{1}]$ ($r^2 = 0.9992$); $A_{MeCN} = 64.6 \times [\mathbf{1}]$ ($r^2 = 0.9999$).

CHART 1

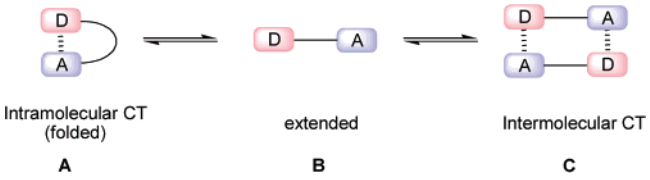

1 and 2. Fluorescence spectra of the CT-dyad **1** (0.1 mM) were measured in dichloromethane at various temperatures (Figure S3, top, left). At 25 °C, a fluorescence spectrum centered at 373 nm was obtained upon excitation at 330 nm. The fluorescence intensity of **1** was much weaker than that of the parent donor compound, that is, 2,6-dimethoxynaphthalene (Figure S2, left), most probably a result of the effective intramolecular quenching by the acceptor moiety in **1** through electron transfer.[20] Interestingly, the temperature dependence of the fluorescence intensity was not monotonical over the temperature range examined, exhibiting an initial increase (from 25 to −35 °C) and a decrease thereafter (to −95 °C). Simultaneously, gradual spectral broadening, particularly in the short-wavelength region, occurred to give a clear shoulder at 367 nm at lower temperatures. In acetonitrile, the fluorescence intensity similarly increased by lowering the temperature down to −40 °C (further cooling was not possible as a result of the freezing of the solvent), and a new emission band at a shorter wavelength was also observed at low temperatures (Figure S2, right). A more concentrated dichloromethane solution of **1** (1 mM) showed clearer differences in the fluorescence spectra at 25 °C and −95 °C (Figure S3, top, right), where two discrete emission maxima at 362 and 373 nm are seen at the latter temperature. In accordance with this, the excitation spectra at the two temperatures disagreed, revealing different relative intensities between the two ^1L_b transitions at 345 and 330 nm. This is rationalized by assuming at least two ground-state conformers for **1**. Thus, the low-energy conformer, absorbing at longer wavelengths, gives fluorescence at shorter wavelengths with a small Stokes shift, while the high-energy or less-stable one, absorbing at shorter wavelengths, fluoresces at longer wavelengths with a large Stokes shift and becomes dominant at high temperatures.[21] Such a contribution was more clearly seen in the relative intensities of the emission of **1** at a different wavelength and in the excitation spectra (Figure S3, bottom). Although details are not discussed here, completely consistent phenomena in the dynamic behavior of the excited state of **2** were also observed (Figures S4 and S5).

The above discussion is also supported by the three-dimensional (3D) representations of the fluorescence spectral behavior of **1** in dichloromethane at two different temperatures (Figure S6). In the two excitation spectra (a and b) obtained at 25 and −95 °C, the peak at 250 nm is consistently seen irrespective of the monitoring wavelength over 340−400 nm, whereas the low-energy peak at 300 nm starts to deviate to longer wavelengths, particularly at longer monitoring wavelengths of 380−400 nm, still preserving the original peak at 300 nm with a much-reduced intensity. Although the spectral shape is roughly coincident with the absorption spectrum, the global spectral pattern is considerably altered. The shape change is more evident in the 3D emission spectra (c and d) obtained at −95 and 25 °C. The relative intensity of the two emission peaks significantly varies and is even inverted at −95 °C by changing the excitation wavelength. These observations are totally compatible with the proposal that at least two conformations, existing in the ground state, are excited in a ratio determined by the solvent, concentration, temperature, and excitation wavelength employed. A very similar tendency is seen with the methyl analogue **2** (Figure S7).

(20) White, R. C.; Buckles, R. E. *J. Photochem.* **1978**, *8*, 67−71.

(21) For similar temperature-dependent fluorescence behavior by conformational changes, see: Mori, T.; Weiss, R. G.; Inoue, Y. *J. Am. Chem. Soc.* **2004**, *126*, 8961−8975.

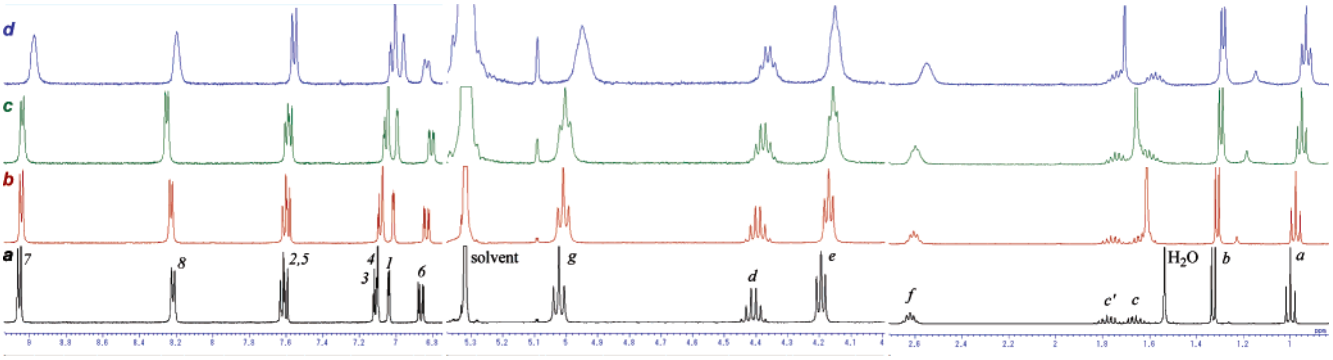

FIGURE 3. ^{1}H NMR spectra of CT-dyad **1** in dichloromethane-d_2 at (a) black, 25 °C; (b) red, −10 °C; (c) green, −50 °C; and (d) blue, −80 °C. For an assignment of protons, see Chart 2.

Fluorescence via CT Band Excitation and Exciplex Emission. A careful examination of the temperature dependence of the fluorescence spectrum of **1** (0.1 mM) in dichloromethane revealed that a weak broad peak emerges at 480−600 nm at low temperatures, which is more clearly seen in the difference spectra obtained by subtracting the normalized spectrum of **1** at 25 °C from those at low temperatures (Figure S8). The weak emission centered at 520 nm is tentatively assigned to exciplex fluorescence from the CT complex. Similar temperature-dependent fluorescence has been reported for trimethylene-bridged 9,10-dicyanoanthracene-naphthalene dyads in 3-methylpentane at much lower temperatures.[22] Others[23] and ourselves[9] have demonstrated that the conventional exciplex and the excited CT complex, generated from a donor−acceptor pair, are unambiguously different in structure and reactivity. In particular, the use of chiral photoreaction serves as a convenient, powerful tool for discriminating these two apparently resembling excited-state species, as exemplified by the distinctly different diastereomeric excesses obtained in the photocycloaddition of stilbene to chiral fumarate upon direct versus CT excitation.[9] Hence, the excitation of the ground-state CT band at 420 nm was examined with the present dyad at low concentration (where contamination by intermolecular association can be avoided) to give moderately intense fluorescence at 520 nm (Figure S8). The fluorescence excitation spectrum monitored at 520 nm displayed a broad band around 400 nm, which is clearly different from the UV−vis spectrum and, hence, assignable to the intramolecular CT absorption. This means that we can clearly distinguish the exciplex and the excited CT complex by means of the fluorescence spectral behavior.

VT-NMR Examinations of the Conformation of CT-Dyad 1. To further elucidate the conformational behavior of the CT-dyad **1** in solution, CT-dyad **1** was examined by a variety of one- and two-dimensional (2D) NMR techniques, including DQF−COSY and ROESY (Figure S9). Small cross-peaks were detected between the naphthalene and the pyridinium protons, indicating that the two aromatic moieties dynamically approach each other, most probably in the folded CT conformation **A** (Chart 1). Then, ^{1}H NMR spectra of **1** were measured in dichloromethane-d_2 at various temperatures (Figure 3 and Chart 2). As the temperature decreases from 25 to −50 °C, most of the protons gradually shift to the upper field with accompanying line broadening, while the pyridinium protons show slight downfield shifts. This is most likely due to the conformational fixation of **1** in the NMR time scale at lower temperatures. However, the spectral changes became discontinuous below −50 °C. For instance, the pyridinium protons are suddenly upfield-shifted and suffer line broadening at −80 °C. This is attributable to the switching of the dominant species in the solution from monomer to dimer around this temperature (vide infra). In the dimer, the naphthyl ring current drives the protons of the facing pyridinium upfield, and the conformational fixation, indicated by DFT calculations (vide infra), may induce the sudden signal broadening. However, we resigned further VT-NMR studies of the conformation of **1** in solution as a result of the low solubility, especially at low temperatures, and the large differences in relaxation time between the naphthyl and the pyridinium protons.

CHART 2

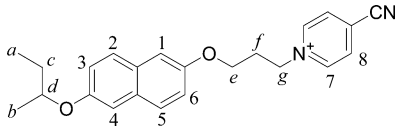

Circular Dichroism Spectra and Anisotropy (*g*) Factor of CT-dyad 1. Circular dichroism spectra were measured for the 3 mM acetonitrile solution of CT-dyad **1** at 25 °C (Figure 4). A cell of 0.2 cm was employed for measuring the Cotton effect at the naphthalene ^1L_b transition, and a molar circular dichroism ($\Delta\epsilon$) of 0.22 was obtained. This is a typical value for a substituted aromatic compound, and the positive Cotton effect is in accordance with the known benzene sector and the benzene chirality rules.[24] Although the ECD intensity of the CT transition was 2 orders of magnitude smaller than those of the ^1L_b transitions, the spectrum could be measured by using a longer cylindrical cell (path length = 10 cm). The *g* factor profile of CT-dyad **1** was accurately determined over the whole spectral range by combining the data obtained under two different conditions (Figure 4, right). The *g* factor of the CT transition thus obtained is comparable to that of the ^1L_b transition.

Variable-temperature ECD spectra of dilute (1 mM) and concentrated (10 mM) solutions (Figure S10) were taken in a conventional 1-cm cell, using a Unisoku cryostat. The $\Delta\epsilon$ values of the ^1L_b and CT bands became more or less larger by lowering the temperature, and the *g* factors showed similar behavior. This enhancement in $\Delta\epsilon$ and *g* is attributable not to an increased

(22) Itoh, M.; Miura, T.; Usui, H.; Okamoto, T. *J. Am. Chem. Soc.* **1973**, *95*, 4388−4392.

(23) (a) Levy, D.; Arnold, B. R. *J. Am. Chem. Soc.* **2004**, *126*, 10727−10731. (b) Irie, M.; Tomimoto, S.; Hayashi, K. *J. Phys. Chem.* **1972**, *76*, 1419−1424. (c) Mataga, N.; Murata, Y. *J. Am. Chem. Soc.* **1969**, *91*, 3144−3152.

(24) Smith, H. E. *Chem. Rev.* **1998**, *98*, 1709−1740.

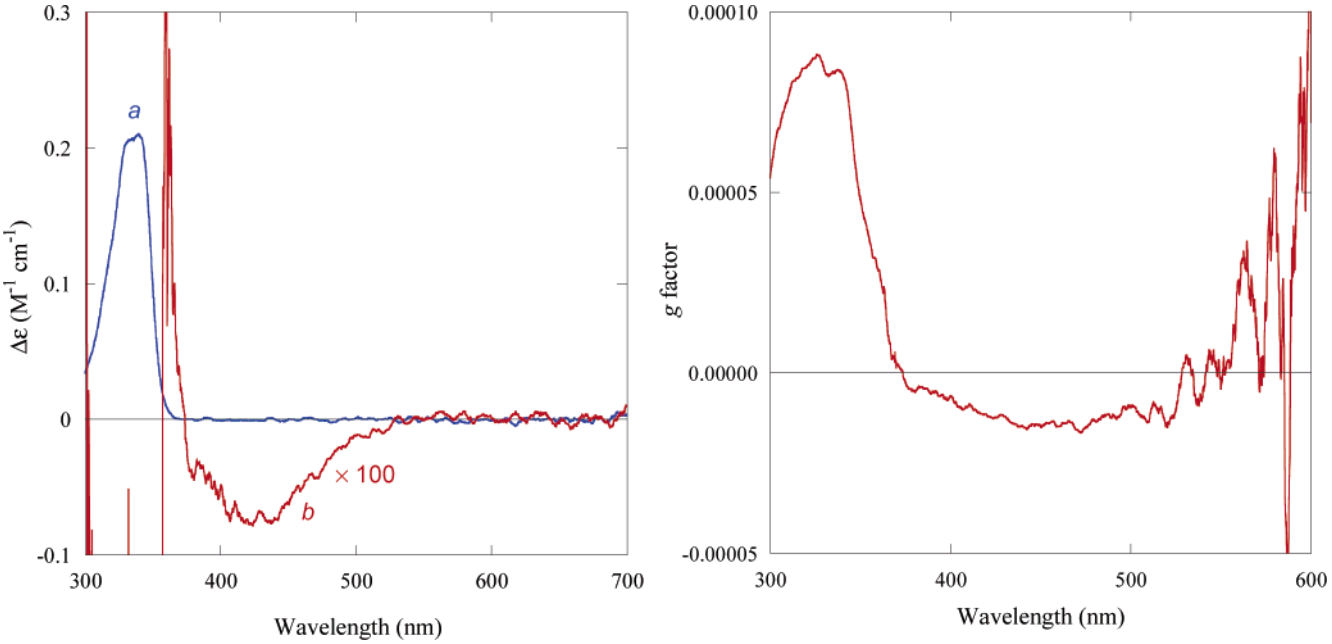

FIGURE 4. Left: circular dichroism spectra of a 3 mM acetonitrile solution of **1** at 25 °C. (a) Path length = 0.2 cm. (b) Path length = 10 cm. Right: *g* factor profile of **1**. Note that the spectrum merged at 370 nm.

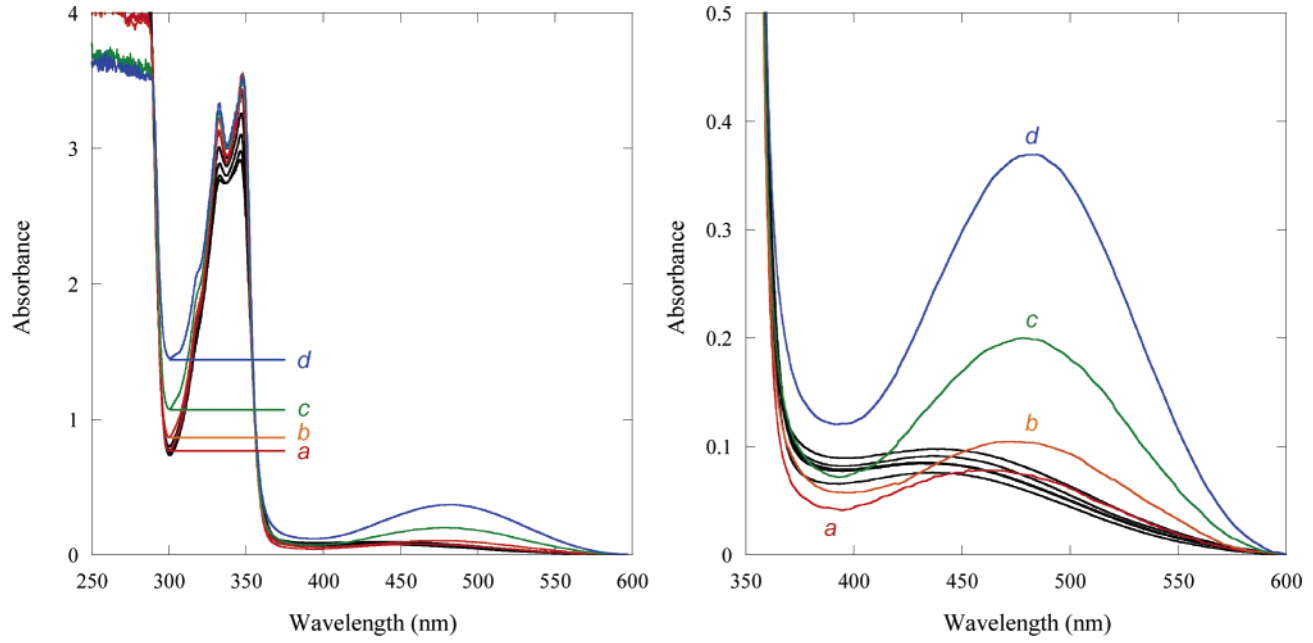

FIGURE 5. Absorption spectra of a 1 mM dichloromethane solution of **1** at 25; 10; −5; −20; −35; (a) red, −50; (b) orange, −65; (c) green, −80; and (d) blue, −95 °C. Right figure is an expansion (× 12.5) of the CT band region.

amount of the folded CT complex at low temperatures, but rather to the conformational fixation of **1**. To the best of our knowledge, the *g* factors on the order of 10^{-4} have not been reported previously for a CT transition.[10,24]

Dimeric CT Complex Formation at Low Temperatures. UV−Vis Spectral Analysis. As mentioned above, we encountered an unanticipated temperature-dependent behavior of the fluorescence and NMR spectra of the chiral CT-dyad **1**. This was more clearly seen in the UV−vis spectrum at lower temperatures, which enabled us to more quantitatively analyze this phenomenon. By decreasing the temperature of a 1 mM dichloromethane solution of **1** to <−50 °C, a new broad absorption band centered at about 480 nm emerged with a slight increase at about 300 nm, at the expense of the intensity of the intramolecular CT band at 420 nm (Figure 5). We could not clearly see such behavior in the case of the achiral analogue **2** (at least up to 0.2 mM), probably a result of the lower solubility of **2** in dichloromethane at the same temperatures.

The absorbances at the peak maxima (480 nm) and also at the half-peak height (520 nm; simply to check the possible contribution of the tail absorption of the intramolecular CT

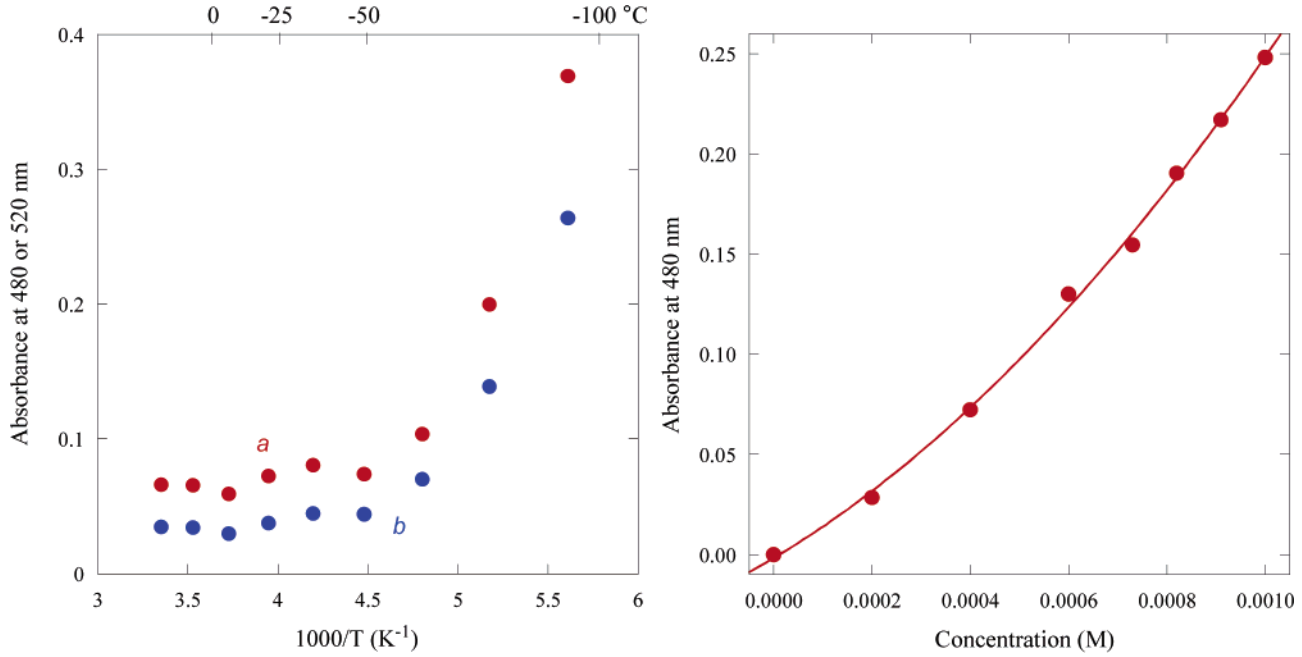

FIGURE 6. Left: temperature dependence of the absorption at (a) 480 and (b) 520 nm. Right: absorbance of the dimeric CT complex (at 480 nm) as a function of the concentration of **1** in dichloromethane at −95 °C. The red line is the nonliner least-squares fit.

TABLE 1. Estimated Electronic Coupling Elements in Various Conformations of CT-dyad 1, Calculated by the Mulliken−Hush Equation

CT species	conditions	ν_{max}[a] (10^3 cm^{-1})	$\Delta\nu_{1/2}$[b] (10^3 cm^{-1})	ϵ_{CT}[c] (M^{-1}cm^{-1})	H_{ab}[d] (cm^{-1})
intermolecular CT	MeCN, 25 °C	23.2	6.1	450	1470
folded monomer	MeCN, 25 °C, 10 mM	25.7	7.3	65[e]	650
head-to-tail dimer	CH_2Cl_2, −95 °C, 1.0 mM	21.1	4.9	430[e]	1230
α-CD complex	H_2O, 25 °C, 1.0 mM, α-CD (5.0 mM)	25.0	6.5	130[e]	860
β-CD complex	H_2O, 25 °C, 1.0 mM, *β*-CD (5.0 mM)	27.1	7.1	220[e]	1200
γ −CD complex	H_2O, 25 °C, 1.0 mM, *γ*-CD (5.0 mM)	28.4	9.7	160[e]	1220
Me−*β*-CD complex	H_2O, 25 °C, 1.0 mM, Me_3−*β*-CD (5.0 mM)	27.4	9.6	110[e]	990
Me−*γ*-CD complex	H_2O, 25 °C, 1.0 mM, Me_3−*γ*-CD (5.0 mM)	26.2	8.6	100[e]	890
CB[8] complex	D_2O, 25 °C, 0.3 mM, CB[8] (0.33 mM)	20.7	5.3	200[e]	870

[a] Absorption maxima at CT band, obtained by deconvolution of the absorption spectra. [b] Band full width at half-height. [c] Molar extinction coefficient at the CT absorption maxima. [d] Electronic coupling element, assuming separation distance as 3.5 Å. See text for details. [e] The value was obtained for a mixture of conformers and estimated by assuming quantitative formation of the CT complex at the given conditions.

complex) were plotted against the reciprocal temperature. As can be seen from Figure 6 (left), the new band becomes appreciable at about −40 °C. The absorption at 480 nm was highly concentration dependent in dichloromethane at −95 °C to give a nonlinear profile, which was fitted to a second-order equation by nonlinear least-squares curve fitting:

$$A_{CT} = \frac{\epsilon_{CT}}{2}\sqrt{\left(2C + \frac{1}{K_{CT}}\right) - \left(2C + \frac{1}{K_{CT}}\right)^2 - 4C^2}$$

From the fitting parameters obtained, the equilibrium constant for the dimer formation and the extinction coefficient of the new species were evaluated: $K_{CT} = 3160 \pm 970$ (M^{-1}) and $\epsilon_{CT} = 427 \pm 39$ (M^{-1} cm^{-1}). Taking into account the spectroscopic observations of the new broad band in the visible region with a moderate extinction coefficient obtained above, we may conclude that the dimeric CT complex (form **C** in Chart 1) is the conformation of this new species. A head-to-tail orientation should be preferred, as supported by a DFT calculation and electronic coupling element values (vide infra).

Intra- and Intermolecular Electron Transfer in Monomeric and Dimeric CT Complexes. An Analysis of the Mulliken−Hush Theory. As has been pointed out by Hush, Marcus, and Sutin, the CT transition reflects the electronic coupling element according to the following relationship:[25]

$$H_{ab}\,(\text{cm}^{-1}) = 0.0206 \times \frac{\sqrt{\nu_{max}\Delta\nu_{1/2}\epsilon_{CT}}}{r_{DA}}$$

where ν_{max} and $\Delta\nu_{1/2}$ are the maximum and full width at the half heights of the (deconvoluted) visible absorption band, ϵ_{CT} is the molar extinction coefficient (in M^{-1} cm^{-1}) at the CT band maximum, and r_{DA} is the effective separation of redox centers in the complex (in Å). We assume that r_{DA} equals 3.5 Å in the Hush equation on the basis of the X-ray crystallographic data

(25) (a) Marcus, R. A.; Sutin, N. *Biochim. Biophys. Acta* **1985**, *811*, 265−322. (b) Hush, N. S. *Coord. Chem. Rev.* **1985**, *64*, 135−157. (c) Hush, N. S. *Electrochim. Acta* **1968**, *13*, 1005−1023. (d) Hush, N. S. *Prog. Inorg. Chem.* **1967**, *8*, 391−444. (e) Hush, N. S. *Trans. Faraday Soc.* **1961**, *57*, 557−580.

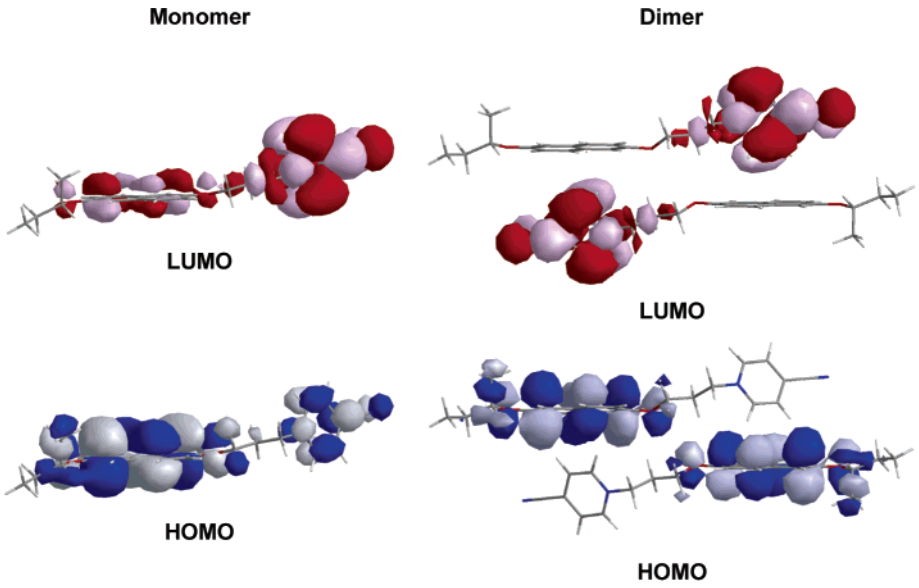

FIGURE 7. B3LYP/6-31G(d)-optimized structures of the monomeric and dimeric forms of **1** and their HOMO and LUMO.

TABLE 2. Calculated Parameters of the Monomeric and Dimeric Forms of 1

	1		**2**	
	monomer	dimer	monomer	dimer
optimized energy[a] (hartree)	−1151.2041	−2302.3839	−1151.2041	−2302.3839
energy difference[b] (kJ/mol)	≡ 0	+0.50	≡ 0	+0.50
dipole moment (debye)	18.48	5.38	18.48	5.38
partial charge on pyridinium[c]	+0.524	+0.579	+0.433	+0.579
partial charge on trimethylene[c]	+0.567	+0.571	+0.560	+0.571
partial charge on naphthalene[c]	−0.091	−0.150	+0.007	−0.152
degree of charge transfer	19%	2 × 14 = 28%	29%	2 × 14 = 28%

[a] Optimized SCF energy at the B3LYP/6-31G(d) level and not corrected by zero-point energy. [b] Calculated as E (dimer) − 2 × E (monomer). [c] Sum of Mulliken charges.

and the DFT-optimized structure of relevant CT complexes.[26] As shown in Table 1, the electronic coupling element H_{ab} calculated for the folded monomer (**A**) is 650 cm^{-1}, which is comparable to, or slightly smaller than those of known CT complexes.[27] It should be noted that the H_{ab} value of the dimeric form (**C**) is almost twice as large as that of the monomer (**A**), indicating that the two sets of donor−acceptor interactions are operating almost independently in the dimeric CT complex. It is also likely that such dual CT interactions inevitably cause conformational restrictions in the resulting complex, as revealed by the increased ECD intensities (vide infra).

DFT Optimization of the Monomeric and Dimeric Forms of CT-Dyad 1. DFT calculations[28] at the B3LYP/6-31G(d) level of the monomeric donor−acceptor system **1** were carried out for a number of conformations.[29] It was found that the most stable conformer at this level of theory has an extended structure in which the naphthalene and pyridinium faces are positioned perpendicular to each other and the two alkoxy groups attached to naphthalene are syn to each other. The other optimized conformers, such as the extended conformation with anti orientation with respect to the alkoxy groups or the partially folded conformation, have similar stabilities ($\Delta E \leq 5$ kJ/mol).

In the one of the DFT-optimized dimer complexes of **1**, two CT-dyad molecules are oriented head-to-tail, and interestingly, the facing naphthalene and pyridinium moieties are not parallel, but perpendicular to each other, as illustrated in Figure 7. The obtained structure is favored in terms of the all-gauche conformation of the trimethylene linker, as well as the minimal π-electron repulsion between the donor and the acceptor moieties. The very small calculated energy difference (0.5 kJ/mol) between the dimer and two monomer molecules and the much smaller calculated dipole moment of the dimer (Table 2) readily leads the system to the preferential dimer formation in less-polar solvents at lower temperatures. The HOMO and LUMO lobes of the optimized monomer and dimer are also shown in Figure 7. In both cases, the HOMO−LUMO transition can be considered the charge transfer from the naphthalene to the pyridinium, but the lobes are more localized in the dimer. The calculated degree of charge transfer in the dimer (2 × 14% = 28%) is much larger than in the monomer (19%). Unfortu-

(26) (a) Yoshikawa, H.; Nishikiori, S.-i.; Ishida, T. *J. Phys. Chem. B* **2003**, *107*, 9261−9267. (b) Liao, M.-S.; Lu, Y.; Scheiner, S. *J. Comput. Chem.* **2003**, *24*, 623−631.

(27) (a) Sun, D.-L.; Rosokha, S. V.; Lindeman, S. V.; Kochi, J. K. *J. Am. Chem. Soc.* **2003**, *125*, 15950−15963. (b) Lindeman, S. V.; Hecht, J.; Kochi, J. K. *J. Am. Chem. Soc.* **2003**, *125*, 11597−11606. (c) Lindeman, S. V.; Rosokha, S. V.; Sun, D.; Kochi, J. K. *J. Am. Chem. Soc.* **2002**, *124*, 843−855.

(28) (a) Becke, A. D. *J. Chem. Phys.* **1993**, *98*, 5648−5652. (b) Parr, R. G.; Yang, W. *Density-Functional Theory of Atoms and Molecules*; Oxford University Press: Oxford, 1989. (c) Hohenberg, P.; Kohn, W. *Phys. Rev. B: Condens. Matter* **1964**, *136*, 864−871. (d) Kohn, W.; Sham, L. J. *Phys. Rev. A: At., Mol., Opt. Phys.* **1965**, *140*, 1133−1138.

(29) Details of (TD)DFT calculations with a higher level of theory will be published elsewhere. See Supporting Information for all optimized geometries at the B3LYP/6-31G(d) level.

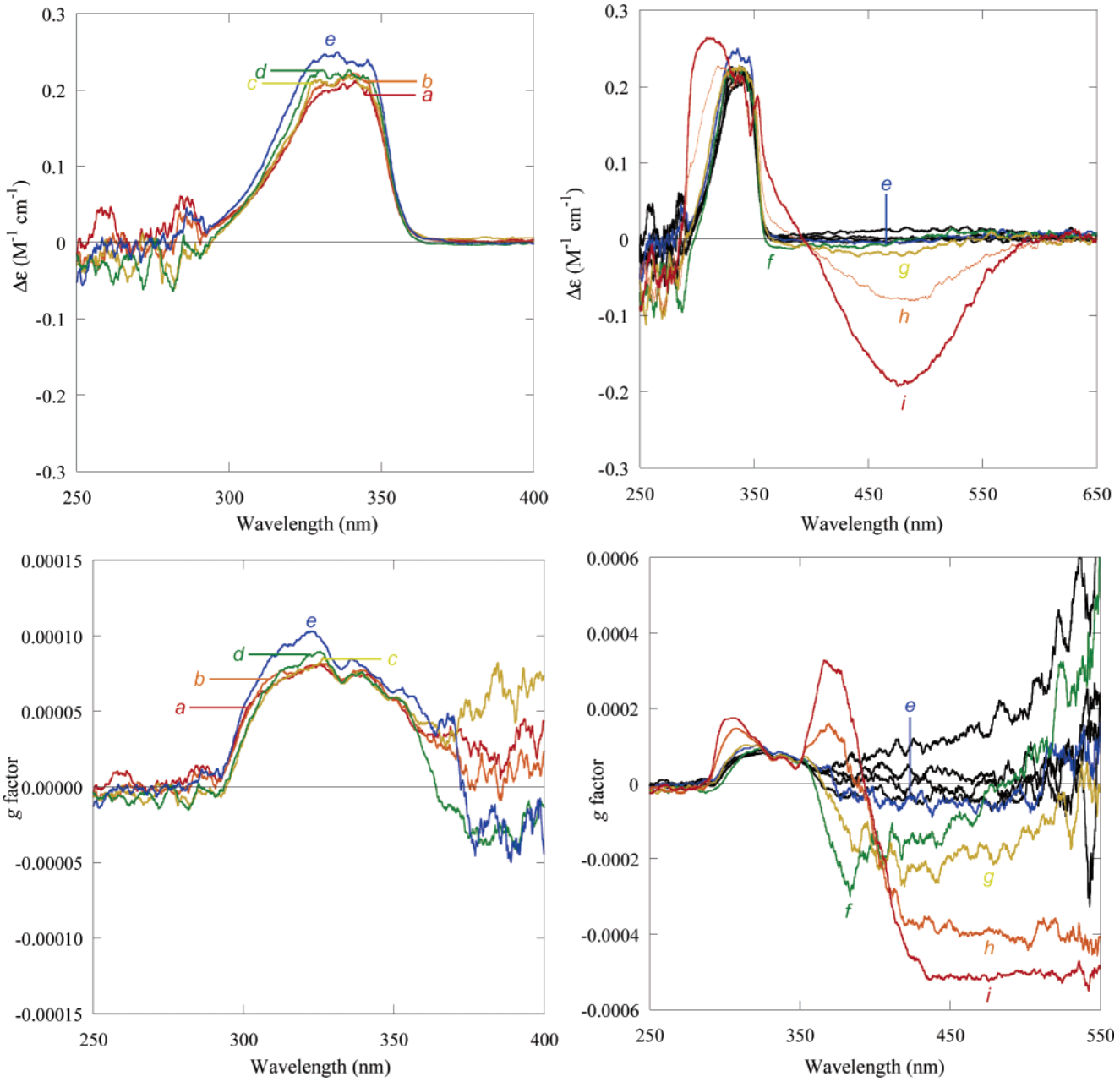

FIGURE 8. Circular dichroism spectra (top) and *g* factors (bottom) obtained with 1.0 mM of **1** in dichloromethane at different temperatures. Left: (a) red, 25 °C; (b) orange, 10 °C; (c) yellow, −5 °C; (d) green, −20 °C; and (e) blue, −35 °C. Right: black, 25 to −20 °C; (e) blue, −35 °C; (f) green, −50 °C; (g) yellow, −65 °C; (h) orange, −80 °C; and (i) red, −95 °C.

nately, B3LYP/6-31G(d) optimization of the folded conformer in the face-to-face naphthalene−pyridinium orientation was consistently unsuccessful, probably due to the overestimation of the electronic interactions between donor and acceptor in this level of theory.[30]

Circular Dichroism Spectra of the Dimeric CT Complex of 1. In general, circular dichroism spectra are not very sensitive to temperature, merely reflecting the degree of conformational fixation at low temperatures. Thus, the molar ellipticity of most chiral organic molecules increases more or less by lowering the temperature. This was indeed the case with the circular dichroism of the folded conformation of **1**; see the spectra in dichloromethane at 25 to −35 °C (Figure 8, left) and in acetonitrile (40 to −40 °C, Figure S10). The absolute values of $\Delta\epsilon$ and the *g* factor were increased by lowering the temperature (at least to −40 °C), but the degree of the enhancement was <5%. At much lower temperatures, where dimeric species become dominant, the *g* factor was dramatically enhanced, as shown in Figure 8 (right). Thus, the new Cotton effect peaks rapidly grew at 480, 380 (sh), and 320 nm as the temperature of a dichloromethane solution of **1** was lowered from −35 to −95 °C. The broad absorption at 480 nm with a negative Cotton effect is assigned to an intermolecular CT transition of the dimeric form of **1**. Such a large temperature dependence of the circular dichroism is not solely attributed to an increased formation of the dimer by lowering the temperature but also to

(30) See, for example: Grimme, S. *Chem.—Eur. J.* **2004**, *10*, 3423−3429 and references therein.

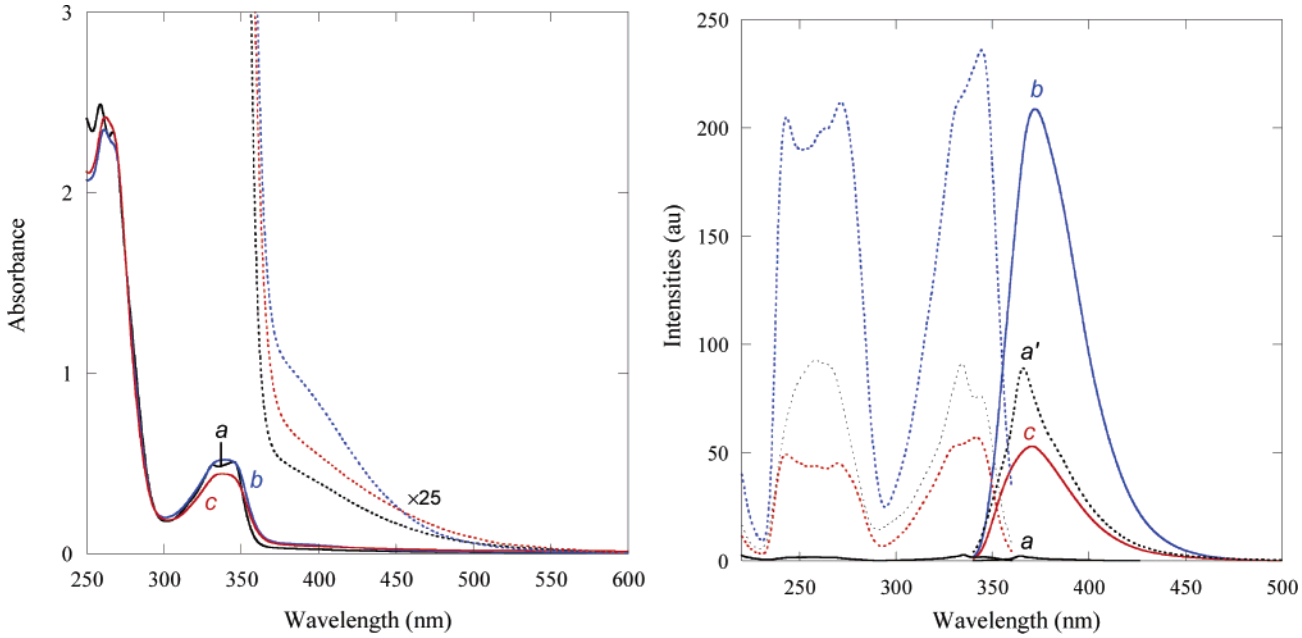

FIGURE 9. Left: absorption spectra of **1** (1 mM) at 25 °C (a) in methanol and (b) in the presence of β- and (c) γ-CD (5 mM) in water. Right: fluorescence and fluorescence excitation spectra of **1** (0.1 mM) at 25 °C (a) in methanol; (a′) in methanol with wider slit widths (excitation, 5 nm; emission, 5 nm instead of 3 × 3 nm); and (b) in the presence of β- and (c) γ-CD (0.5 mM) in water.

an enhancement of the anisotropy at low temperatures. Indeed, the *g* factor, which is already corrected for the increase in the dimer concentration, is enhanced significantly, as can be seen from Figure 8 (bottom right). It is noteworthy that the *g* factor of the intermolecular CT transition (420−550 nm) gradually gave larger negative values on lowering the temperature, whereas the *g* factor at 350−380 nm, which is almost 0 at 25 °C, first went to the negative side (25 to −65 °C) and then turned to the positive side (−80 to −95 °C). This is because the Cotton effect of the monomer's CT band is progressively replaced by the Cotton effect of the CT band of the dimer in this region. It is quite interesting that, due to the conformational fixation of the chiral group by stronger interactions in the dimer, the *g* factor of the dimer CT complex is significantly enhanced, particularly at lower temperatures ($g = -5.2 \times 10^{-4}$ at −95 °C) compared to that of the monomer ($g = -1.6 \times 10^{-5}$ at 25 °C).

Effects of Confinement on Circular Dichroism of CT Complexes. *β*- and *γ*-CD Cavities. The photophysics and photochemistry of inclusion complexes with CDs have been extensively studied.[31] In the present case, the hydrophobic interactions of CT-dyads **1** and **2** with a CD cavity are expected to occur preferentially at the neutral naphthalene moiety rather than at the positively charged pyridinium moiety. The inclusion of the donor naphthalene moiety of the CT-dyad strongly interrupts the intramolecular CT interactions and, hence, the folded conformation is highly disfavored. In contrast, the extended CT-dyad is expected to form a dimeric CT complex if the host cavity is large enough to accommodate a pair of donor−acceptor moieties. We, therefore, investigated the induced circular dichroism, UV−vis absorption, and fluorescence spectra of **1** and its achiral analogue **2** in the presence of β- and γ-CDs.

UV−Vis Absorption and Fluorescence Spectral Changes of 1 and 2 in the Presence of *β*- and *γ*-CDs. CT-dyad **1**, though completely insoluble in water, could be solubilized by adding an equimolar amount of β- or γ-CD, most probably through the 1:1 (or 2:2) complex formation. The UV−vis spectra of **1** in the presence of 5 equiv of β- and γ-CDs (to ensure the complexation) in water are shown in Figure 9, left (Figure S11 for **2**), which are compared with those in methanol (without CDs).

The UV−vis spectra of **1** in the presence of CDs were similar in shape to those of free **1** in methanol, where the naphthyl moiety absorbs at 330−350 nm and the pyridinium moiety absorbs at about 270 nm. The band structure of the naphthalene's ^1L_b transition, which is clearly seen in methanol (trace a in Figure 9, left), almost disappeared in the spectra of the CD complexes (traces b and c in Figure 9, left), probably due to the substantial interactions of the naphthyl moiety with the CD cavity. A weak but appreciable broad absorption was observed at 370−500 nm as a tail, which is assignable to the intramolecular CT band of the complex. Band deconvolution, however, revealed that the CT band peak of the complex is significantly blue-shifted compared with that of free **1** in methanol (Table 1).

As shown in Table 1, the electronic coupling elements of β-CD−**1** and γ-CD−**1** complexes, calculated assuming the same donor−acceptor distance of 3.5 Å, are larger than that of the folded monomer and comparable to that of the dimer. In the cases of polymethylene-linked donor−viologen dyads reported previously,[6,32,33] the intensity of the CT band was reduced upon the addition of CD, which was rationalized by the retarded formation of the folded monomer upon CD inclusion. In the present case, as a result of the less hydrophobic nature of

(31) (a) Ramamurthy, V.; Eaton, D. F. *Acc. Chem. Res.* **1988**, *21*, 300−306. (b) Weiss, R. G.; Ramamurthy, V.; Hammond, G. S. *Acc. Chem. Res.* **1993**, *26*, 530−536. (c) Saenger, W. *Angew. Chem., Int. Ed. Engl.* **1980**, *19*, 344−362.

(32) (a) Yonemura, H.; Kasahara, M.; Saito, H.; Nakamura, H.; Matsuo, T. *J. Phys. Chem.* **1992**, *96*, 5765−5770. (b) Yonemura, H.; Nakamura, H.; Matsuo, T. *Chem. Phys. Lett.* **1989**, *155*, 157−161.

(33) Toki, A.; Yonemura, H.; Matsuo, T. *Bull. Chem. Soc. Jpn.* **1993**, *66*, 3382−3386.

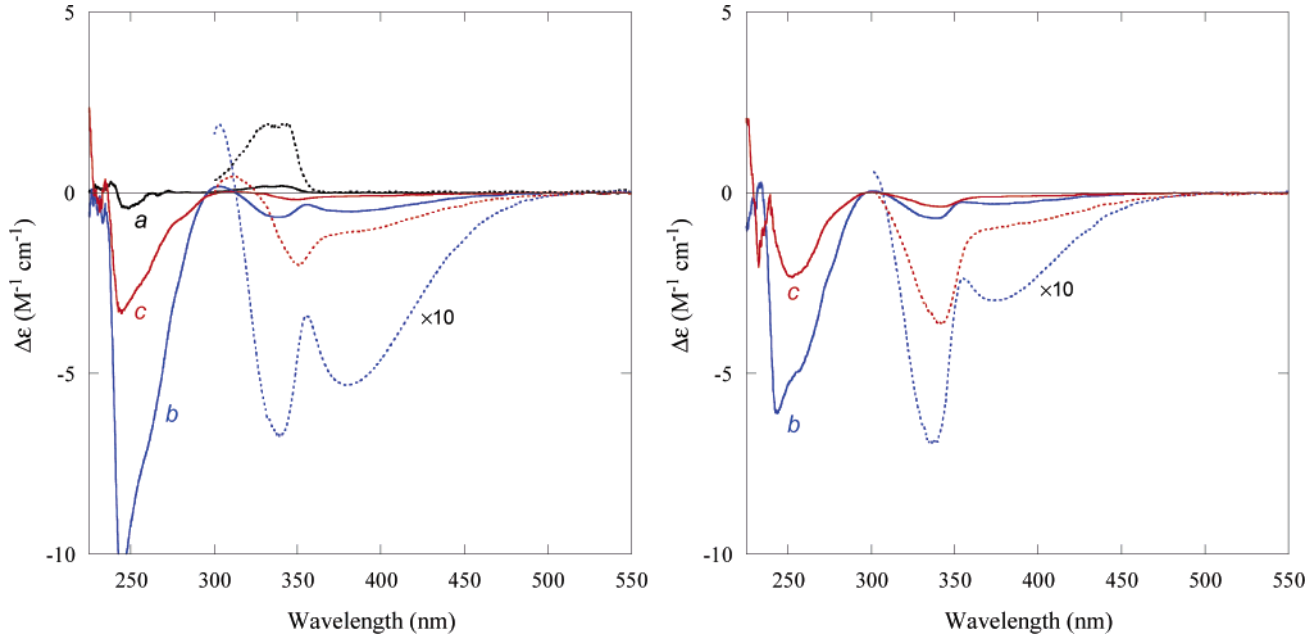

FIGURE 10. Comparison of induced circular dichroism spectra of **1** (left) and **2** (right) (1 mM) at 25 °C (a) in methanol and (b) in the presence of β- or (c) γ-CD (5 mM) in water. Note that two ECD spectra measured by using cells of different path lengths (0.2 cm for 230−300 nm and 1 cm for 300−600 nm) were merged at 300 nm.

pyridinium, as well as the space limitations of the hosts, only the naphthyl moiety of the dyad is thought to interact with the CD cavity (probably from the chiral alkoxyl side). A stronger CT absorption observed upon complexation with CD may be ascribed to the enhanced donor−acceptor interactions in the hydrophobic environment. This idea is supported by the results of induced circular dichroism spectral examinations (vide infra). It is also noted that the enhancement of the CT absorption induced upon complexation is much larger for **1** than for **2**. The larger alkyl group (methylpropyl for **1** versus methyl for **2**) may be responsible, at least in part, for the stronger hydrophobic interaction with CDs and the stronger CT interactions observed in the absorption spectra, which is consistent with the larger electronic coupling element (H_{ab}) for the complex (Table 1).

To gain further insights into the excited-state interactions between **1** and CDs, we investigated the fluorescence spectral behavior of the CD complexes (Figure 9, right, for **1** and Figure S11, right, for **2**). In the presence of β- or γ-CD (5 equiv), an enormous enhancement (more than 100 times) of fluorescence intensity was observed. Virtually the same fluorescence spectral changes were observed for achiral **2**. Similar fluorescence enhancements have been reported for polymethylene-linked carbazole−viologen,[32] anthracene−viologen,[33] and naphthalene−viologen[6] dyads. In the CD−dyad complex, the dynamic quenching by intramolecular CT complexation is avoided to a large degree. The quenching by intermolecular CT formation as well as by solvent attack is also reduced due to the protection of the excited donor molecule in the hydrophobic CD cavity. The smaller β-CD cavity gave better protection to give a larger enhancement of the fluorescence intensity.

Bathochromic shifts of emission maxima (relative to those in methanol, which were used as the references, as the dyads are practically insoluble in water) were observed for both **1** and **2** in the presence of β- and γ-CDs. As can be seen from Table 3, the peak shifts for **1** and **2** are larger upon complexation with β-CD (9 and 7 nm, respectively) than with γ-CD (7 and 5 nm, respectively). Changing the solvent from methanol to less-polar dichloromethane also led to a bathochromic shift of 5 nm, which is similar to those caused by inclusion in CD cavities and, therefore, indicates that the naphthalene moiety is placed in the hydrophobic CD cavity. Judging from the larger bathochromic shift observed for **1**, we may further deduce that the chiral dyad **1** is more deeply and/or tightly fixed in the hydrophobic cavity of γ- and particularly β-CD than the methyl analogue **2**.

TABLE 3. Fluorescence Maxima and Quantum Yields of 1 and 2 in the Presence of Host Molecules[a]

host	equiv	solvent	λ_{max} (**1**), nm	ϕ_{FL} (**1**)	λ_{max} (**2**), nm
none		CH_2Cl_2	373	1.3×10^{-5}	370
		MeOH	365	3.8×10^{-5}	365
α-CD	5.0	H_2O	372	3.4×10^{-5}	
β-CD	5.0	H_2O	374	4.1×10^{-3}	372
γ-CD	5.0	H_2O	372	1.8×10^{-3}	370
Me−β-CD	5.0	H_2O	372	4.2×10^{-3}	
Me−γ-CD	5.0	H_2O	373	9.7×10^{-4}	
CB[8]	1.1	D_2O	399	6.5×10^{-4}	

[a] All fluorescence spectra were recorded for a 0.1 mM solution of **1** or **2** at 25 °C. [b] Fluorescence quantum yields were determined by a comparison with that of 2,6-dimethoxynaphthalene ($\Phi_{FL} = 0.44$).[34]

In methanol, two maxima at 334 and 345 nm with relative intensities of 1.24 were observed in the excitation spectra of **1**, monitored at 370 nm. In the presence of CDs in water, however, the relative intensities of the two maxima were reversed to 0.97 and 0.98 for β- and γ-CDs, respectively. The fluorescence excitation spectra and the UV−vis spectra showed appreciable differences in shape and relative intensity, indicating the existence of several conformations of **1** within the CD cavity.

Comparison of Induced Circular Dichroism Spectra and Anisotropy (*g*) Factors of 1 and 2 in the Presence of *β*- and *γ*-CDs. Induced circular dichroism (ICD) spectral examinations of CT-dyad **1** provide us with more detailed information about the host−guest and donor−acceptor interactions (Figure 10 and Figure S12 for g factors). Both the ^1L_b (∼330 nm) and the ^1L_a (∼270 nm) transitions[35] of the naphthalene chromophore showed

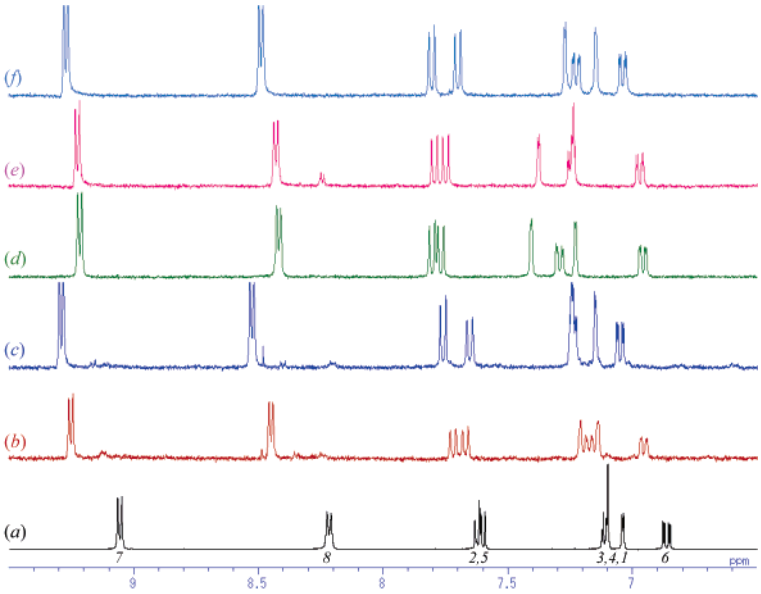

FIGURE 11. Comparison of ^{1}H NMR spectra (aromatic region) of **1** at 25 °C (a) in dichloromethane; in the presence of 5 equiv of (b) γ-CD; (c) β-CD; (d) α-CD; (e) permethylated γ-CD; or (f) permethylated β-CD in D_2O. For the spectra of the alkyl regions, see Figure S13.

CHART 3

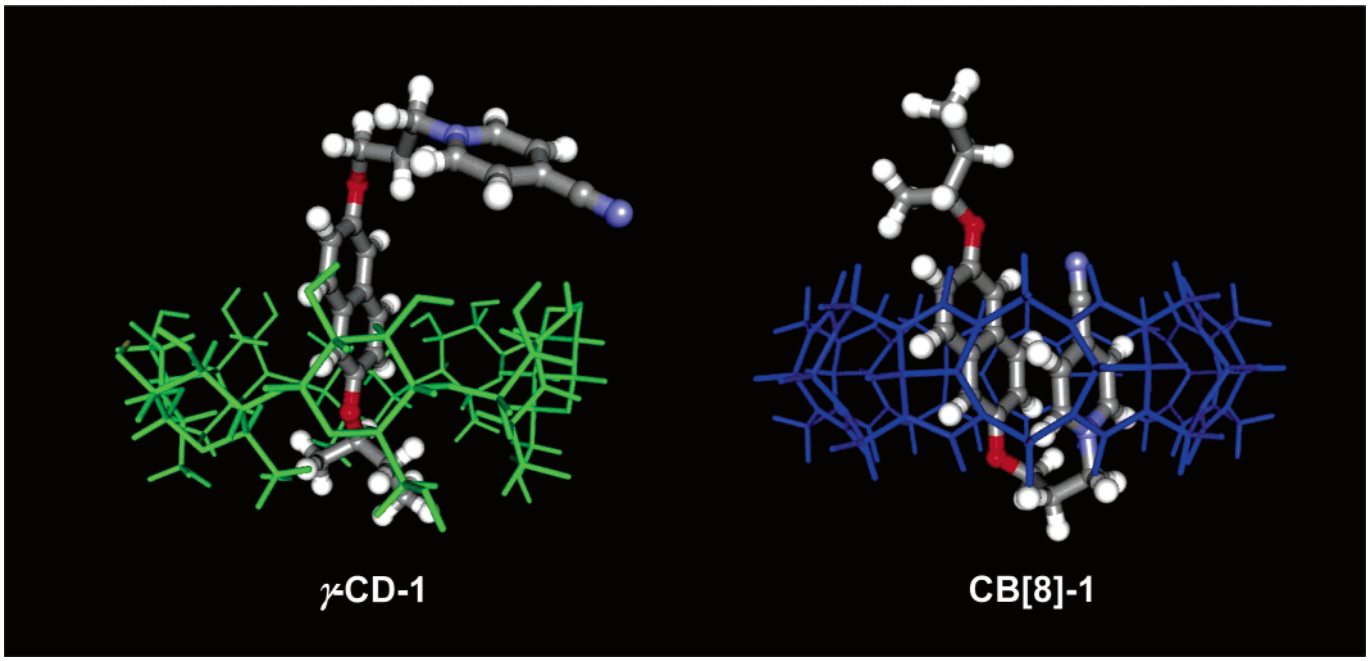

negative ICD. This indicates that the naphthalene's long axis is either penetrating through the CD cavity, as judged from the Harata's rule,[36] or located outside the cavity parallel to the CD rim, as judged from the Kodaka's rule.[37] Interestingly, the CT band also exhibits negative ICD for both **1** and **2**. It is noteworthy that β-CD induces a much stronger Cotton effect than γ-CD, and the ICD intensity is stronger for **1** than for **2** under comparable conditions. The difference in ICD intensities is thought to reflect the degree of fixation of the donor in the CD cavity, as frequently observed for (achiral) naphthalene−CD complexes.[37]

Taking into account all of the spectral evidence, that is, the enhanced fluorescence, the negative Cotton effect for the ^1L_b band, the similar ICD for chiral **1** and achiral **2**, the global ^{1}H NMR deshielding upon complexation (Figure 11 and Figure S13), and the strong CT absorption observed for the inclusion complex, we propose the plausible complexation mode of **1** with the CDs illustrated in Chart 3. The alkoxynaphthyl moiety shallowly penetrates into the CD cavity, and the CT interaction

(34) Sato, C.; Kikuchi, K.; Okamura, K.; Takahashi, Y.; Miyashi, T. *J. Phys. Chem.* **1995**, *99*, 16925−16931.

(35) Note that the negative Cotton effect found at the ^1B_b transition region at about 230 nm was not fully compatible with the known Harata/Kodaka rules. We tentatively assume this was because of the overlap of the multiple transitions at this short wavelength. Further evidence for the structure of the CT-dyad−CD complexes as depicted in Chart 3 was thus obtained from other spectroscopic methods, such as ROESY.

(36) Harata, K.; Uedaira, H. *Bull. Chem. Soc. Jpn.* **1975**, *48*, 375−378.

(37) (a) Kodaka, M. *J. Phys. Chem. A* **1998**, *102*, 8101−8103. (b) Kodaka, M. *J. Am. Chem. Soc.* **1993**, *115*, 3702−3705.

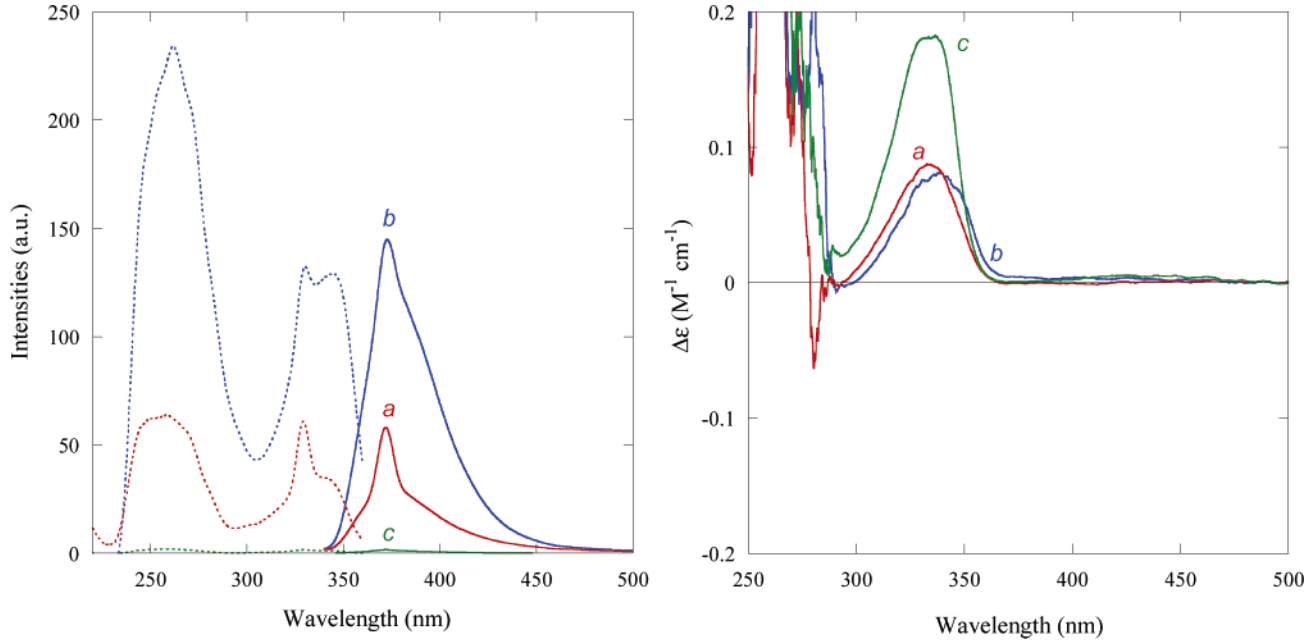

FIGURE 12. Fluorescence (left) and circular dichroism (right) spectra of **1** (1 mM) in water at 25 °C in the presence of 5 equiv of (a) permethylated γ-CD, (b) permethylated β-CD, and (c) native α-CD. Emission spectra excited at 330 nm. Excitation spectra monitored at 400 nm.

with the pyridinium moiety occurs near the portal of the CD. The alternative equatorial orientation inside the cavity is unlikely to occur particularly for β-CD as a result of the cavity size and the steric hindrance of the alkoxynaphthalene group. This mode of complexation occurs probably because of the less-hydrophobic nature of the pyridinium cation. We assume that both the naphthalene moiety and the chiral alkoxyl group are accommodated in the cavity, where the alkoxyl group is located near the CD rim and the naphthalene moiety is shallowly included in the cavity, as shown in Chart 3 (left), while the acceptor moiety (cyanopyridinium) is not included in the cavity. This binding mode still allows dynamic interactions between the donor and the acceptor parts of the dyad to a degree smaller than that experienced by free **1**. Such a complex structure was experimentally supported indeed by the ROESY spectral studies of the β-CD−**1** complex in D_2O at 25 °C (pulse = dante, Figure S14). Briefly, the cross-peaks found between (i) chiral alkoxyl protons (*a*−*d*) and the H_6 of CD, (ii) cyanopyridium (*7*) and the H_1 of CD, and (iii) naphthalene protons (3 and 4) and the H_3, H_5, and H_6 of CD, all support the proposed structure (Chart 3, left).

To the best of our knowledge, this is the first observation of such an anomalously large ICD at the CT band caused by the complexation with CDs.[12] This is more clearly seen in the *g* factors (Figure S12). The *g* factors of -0.8 to -2.8×10^{-3} for allowed CT transitions are unexpectedly large, while the ^1L_b and ^1L_a transitions give smaller *g* factors upon complexation with CDs. Probably, the complexation of the naphthalene moiety reduces the conformational diversity of the CT-dyad, which in turn enhances the anisotropy of the donor-to-acceptor transition. It is noted that the enhancement of the *g* factors of β-CD−**1** and γ-CD−**1** complexes does not uniformly happen to all transitions. Indeed, the inclusion-induced ICD enhancement is more pronounced for the CT transition. Such a technique to enhance the *g* factor of the CT transition by constraints may be used as a convenient powerful tool in the study of absolute asymmetric synthesis with a circularly polarized light.[38]

Other Cyclodextrins. To further explore the scope of the anisotropy enhancement by constraints, we examined other CD derivatives of different sizes and shapes as hosts, that is, native α-CD and permethylated β- and γ-CDs. The permethylated CDs, lacking the intramolecular hydrogen bond network around the wider rim,[39] are known to have more flexible skeletons and expanded hydrophobic cavities. Their complexation behavior with CT-dyad **1** was studied in detail by means of UV−vis (Figure S15, left, and Table 1), fluorescence (Figure 12, left, and Table 3) and ^{1}H NMR spectroscopies (Figure 11 and Figure S13). The CT bands, observed in the UV−vis spectra, clearly indicate the existence of the donor−acceptor interactions in all of the complexes examined, which are considered to be comparable in magnitude to the similar λ_{max}, ϵ_{CT}, and H_{ab} values. Fluorescence intensity was enhanced upon the addition of permethylated β- and γ-CDs, clearly indicating that the formation of the corresponding inclusion complexes with these hosts, while such an enhancement was not observed upon addition of α-CD. However, the addition of α-CD to an aqueous solution of **1** appears to facilitate some interactions between them, as **1** becomes soluble to some extent, probably through partial inclusion of the alkyl group of **1** in the α-CD cavity. Indeed, the observed circular dichroism spectrum was almost identical to that obtained in methanol in the absence of CD (Figure 12, right, and Figure S15, right, for *g* factors). No appreciable Cotton effect was observed at the CT band. Although the fluorescence and ^{1}H NMR spectral evidence clearly indicates that the inclusion complex of **1** is formed with permethylated β- and

(38) (a) Review: Feringa, B. L.; van Delden, R. A. *Angew. Chem., Int. Ed.* **1999**, *38*, 3418−3438. See also: (b) Nishino, H.; Kosaka, A.; Hembury, G. A.; Aoki, F.; Miyauchi, K.; Shitomi, H.; Onuki, H.; Inoue, Y. *J. Am. Chem. Soc.* **2002**, *124*, 11618−11627. (c) Inoue, Y.; Tsuneishi, H.; Hakushi, T.; Yagi, K.; Awazu, K.; Onuki, H. *Chem. Commun.* **1996**, 2627−2628.

(39) (a) Kano, K.; Hasegawa, H. *J. Am. Chem. Soc.* **2001**, *123*, 10616−10627. (b) Ramirez, J.; Ahn, S.; Grigorean, G.; Lebrilla, C. B. *J. Am. Chem. Soc.* **2000**, *122*, 6884−6890.

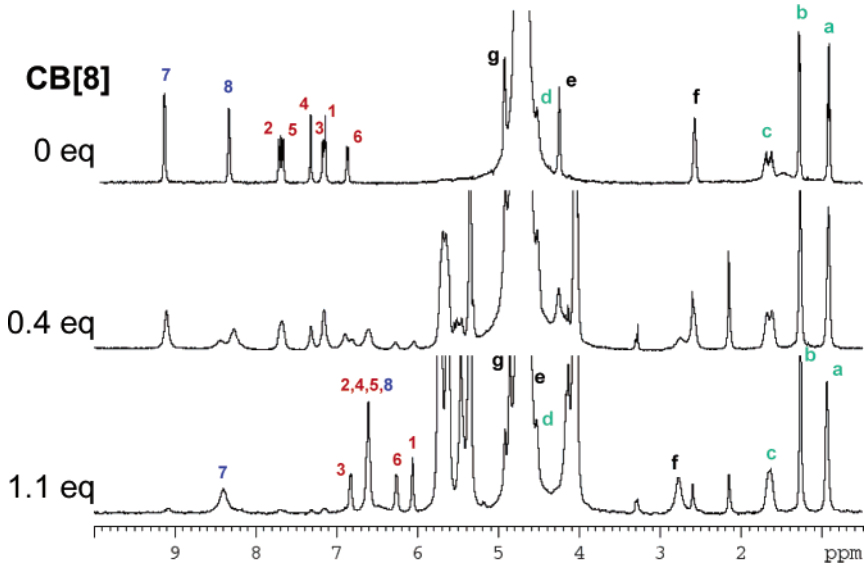

FIGURE 13. Changes of ^{1}H NMR chemical shifts upon the complexation of **1** with CB[8]. For the assignment of protons, see Chart 2.

γ-CDs, the observed circular dichroism spectra were dramatically different from those obtained with the native β- and γ-CD complexes. The Cotton effect at the CT transition was not apparent, and the intensity of the ^1L_b transition was slightly reduced. This may be accounted for in terms of the relatively flexible nature of these hosts, which does not allow the conformational restriction of the chiral group. It has recently been shown that the location of the included guest differs for native and permethylated CD complexes.[40] It is thus demonstrated that the shape, size, and nature of the cavity significantly affect the *g* factor of the CT transition.

Cucurbit[8]uril. Cucurbiturils (CBs) and CDs are known to form inclusion complexes with a variety of organic guest molecules, but they are fundamentally different in their host−guest interactions.[41] CDs bind guests mainly through van der Waals interactions, whereas the carbonyl groups at the portals of CBs allow ion−dipole as well as hydrogen-bonding interactions with guests. The inner surface of the CB cavity is negative, while the outer surface is somewhat positive. On the other hand, the rim and inside of CDs are almost neutral. Consequently, CBs preferentially bind guests with a positive charge, whereas CDs prefer neutral guests. It is also noteworthy that CBs are structurally more rigid than CDs. A comparison of the host−guest interactions and their photoreactions in the cavities of CBs and CDs has been reported very recently by Ramamurthy and co-workers.[42] The host−guest interactions between CB[8] and CT-dyad **1** are expected to be quite different, and it was indeed the case, particularly with the mode of complexation and the effect on the circular dichroism, as described below.

UV−Vis and Fluorescence Spectra of 1 in the Presence of Cucurbit[8]uril. It is known that CBs become more soluble in water in the presence of metal salts, but the association constant of methyl viologen with cucurbit[7]uril is much larger in the absence of competing metal ions.[43] Hence, we performed the following spectroscopic studies in pure water (or D_2O).

Upon the addition of CT-dyad **1** to a saturated solution of CB[8] (ca. 0.3 mM) in D_2O, a pale pink color (λ_{max} = 483 nm) immediately developed (Figure S16, left), indicating donor−acceptor interactions. Assuming complete formation of the folded intramolecular CT complex (vide infra) and the same donor−acceptor distance, the electronic coupling element was estimated as 870 cm^{-1} (Table 1). The value is significantly larger than that of the monomeric CT complex (650 cm^{-1}), showing stronger intramolecular interactions between the donor and the acceptor moieties. In accordance with this, the CT absorption, revealed by the band deconvolution, is bathochromically shifted. Fluorescence spectrum of the CT-dyad **1** complexed with CB[8] displayed a large red shift to 499 nm (Figure S16, right) and an intensity enhancement in comparison with free **1**, the extent of which are, however, much less than those observed for β- and γ-CD complexes (Table 3). The excitation spectrum of the CB[8]−**1** complex was considerably different from that of free **1**, indicating that the fluorescing species is different in structure from the one in solution. It is reasonable that the major folded conformer is statically quenched by intramolecular electron transfer upon excitation, while the minor conformer(s) of **1** complexed with CB[8] can survive to fluoresce.

NMR Spectral Studies of the CB[8]−1 Complex. The CB[8]−**1** complex was further characterized by several NMR methods, including DQF−COSY, ROESY (Figure S9, bottom), and pulsed-field gradient (PFG) techniques (Figure S17, right). Upon the addition of an appropriate (∼equimolar) amount of CT-dyad **1** to a saturated D_2O solution of CB[8], the ^{1}H NMR spectrum of the solution (Figure 13) showed only one set of signals, indicating the quantitative formation of a single complex. All of the pyridinium (7 and 8) and naphthalene (1−6) proton signals shifted upfield relative to those of the free guest, whereas the trimethylene (e and f) proton signals shifted

(40) Mieusset, J.-L.; Krois, D.; Pacar, M.; Brecker, L.; Giester, G.; Brinker, U. H. *Org. Lett.* **2004**, *6*, 1967−1970.

(41) (a) Lee, J. W.; Samal, S.; Selvapalam, N.; Kim, H.-J.; Kim, K. *Acc. Chem. Res.* **2003**, *36*, 621−630. (b) Lagona, J.; Mukhopadhyay, P.; Chakrabarti, S.; Isaacs, L. *Angew. Chem., Int. Ed.* **2005**, *44*, 4844−4870. (c) Gerasko, O. A.; Sokolov, M. N.; Fedin, V. P. *Pure Appl. Chem.* **2004**, *76*, 1633−1646. (d) Kim, K.; Kim, H.-J. In *Encyclopedia of Supramolecular Chemistry*; Atwood, J. L., Steed, J. W., Eds.; Marcel Dekker: New York, 2004; pp 390−397. (e) Marquez, C.; Hudgins, R. R.; Nau, W. M. *J. Am. Chem. Soc.* **2004**, *126*, 5806−5816.

(42) (a) Pattabiraman, M.; Natarajan, A.; Kaanumalle, L. S.; Ramamurthy, V. *Org. Lett.* **2005**, *7*, 529−532. (b) See also: Jon, S. Y.; Ko, Y. H.; Park, S. H.; Kim, H.-J.; Kim, K. *Chem. Commun.* **2001**, 1938−1939.

(43) Ong, W.; Kaifer, A. E. *J. Org. Chem.* **2004**, *69*, 1383−1385.

TABLE 4. Summary of the Effects on *g* Factors via Confinement

CT species	conditions	λ_{max} (CT) (nm)	H_{ab} (cm^{-1})	*g* factor ($\times 10^5$)	enhancement
intermolecular complex	MeCN, 25 °C	420	1470		
folded monomer	MeCN, 25 °C, 10 mM	420	650	−1.6	≡ 1
head-to-tail dimer	CH_2Cl_2, −95 °C, 1.0 mM	480	1230	−52	33
α-CD complex	H_2O, 25 °C, 1.0 mM, α-CD (5.0 mM)	400	860	+2	∼1
β-CD complex	H_2O, 25 °C, 1.0 mM, *β*-CD (5.0 mM)	380	1200	−28	5[b]
γ-CD complex	H_2O, 25 °C, 1.0 mM, *γ*-CD (5.0 mM)	370	1220	−9	∼1[b]
Me−*β*-CD complex	H_2O, 25 °C, 1.0 mM, Me_3−*β*-CD (5.0 mM)	360	990	n.d.[a]	
Me−*γ*-CD complex	H_2O, 25 °C, 1.0 mM, Me_3−*γ*-CD (5.0 mM)	380	890	∼0	∼0
CB[8] complex	D_2O, 25 °C, 0.3 mM, CB[8] (0.33 mM)	480	870	−16	10

[a] Not determined due to significant overlap of ^1L_b transition of **1**. [b] The values were corrected by using the effect of induced circular dichroisms of the chiral CD cavity with **2**.

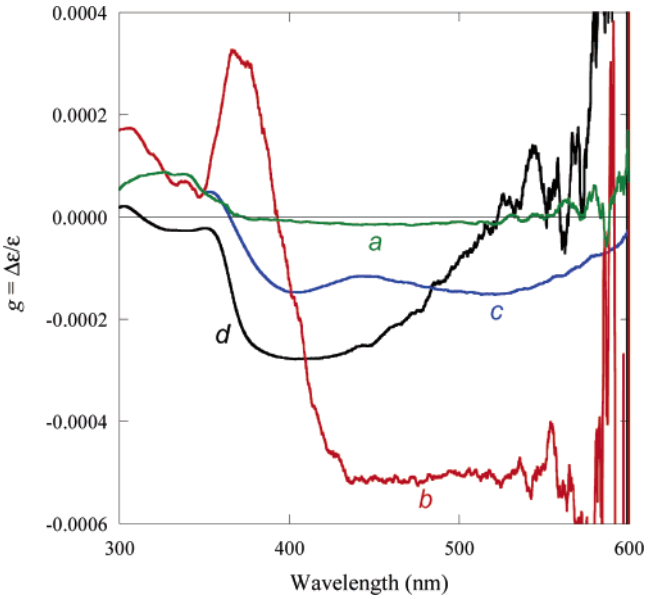

FIGURE 14. Comparison of the *g* factors of the CT transition of **1**. (a) The folded monomer in acetonitrile at 25 °C. (b) The head-to-tail dimer in dichloromethane at −95 °C. (c) The folded conformation in CB[8] in D_2O at 25 °C. (d) The inclusion complex with *β*-CD in H_2O at 25 °C.

downfield. In contrast, the chiral methylpropyl proton signals (a−d) in the complex did not show appreciable shifts. This implies that the two aromatic rings are completely included and stacked with each other inside the CB cavity, while the trimethylene and chiral alkyl groups are sticking out of the cavity in the bulk solution. Other possible interactions, such as the electrostatic interactions of the pyridinium cation and the portal carbonyl of CB[8], may also contribute to the inclusion complexation. Notably, the hydrodynamic volume of the complex, measured by the PFG NMR technique, is only 1.2 times larger than that of CB[8] itself. Taking into account all of these results, we can safely conclude that CT-dyad **1** is folded into the CB[8] cavity to form a tightly packed 1:1 complex, as depicted in Chart 3, right.

Circular Dichroism of the Folded CT Complex in the Cucurbit[8]uril Cavity. The chiroptical properties of the folded CT-dyad **1** included in the CB[8] cavity (form **A** in Chart 1) are of particular interest. Thus, the CB[8]−**1** complex was subjected to the circular dichroism spectral examinations (Figure S17, left), where the anisotropy factor profiles of **1** under a variety of conditions are compared in Figure 14. The circular dichroism spectrum of the CB[8]−**1** complex exhibits a positive Cotton effect at 350 nm, which corresponds to the ^1L_b transition of the naphthalene chromophore, as well as the two extrema at about 400 and 520 nm, both of which are assignable to the $\pi^* \leftarrow a_u$ and $\pi^* \leftarrow b_{1u}$ (intramolecular CT) transitions of the dyad. The hidden transition (HOMO → LUMO or au → π^*) of the CT complex was not observed without confinement. (A similar trend was also observed for the dimer (CH_2Cl_2, −95 °C) for the intermolecular CT). The appearance of the two CT bands is a reflection of the fixed donor−acceptor orientation in the CB[8] cavity. The anisotropy factors of the two CT transitions ($g \sim 10^{-4}$) are within a range of the known allowed transitions, but are about 20 times larger than that of the folded monomer at the same temperature (Table 4). Confining CT-dyad **1** in CB[8] greatly enhances the anisotropy of the CT transition, probably through the fixation of the donor−acceptor orientation, as illustrated in Chart 3. It is thus concluded that both the orientational fixation of the relevant donor and acceptor and the conformational fixation of the chiral group are equally essential for obtaining a larger *g* factor of the CT band.

Summary and Conclusions

We have prepared new CT-dyad systems (**1** and **2**) composed of a 2,6-alkoxynaphthalene donor, trimethylene linker, and a 4-cyanopyridinium acceptor. The dynamic behavior of these dyads, that is, the intramolecular versus the intermolecular CT complexation, has been studied by means of UV−vis, fluorescence, and NMR spectroscopies in acetonitrile and dichloromethane. We found that the intramolecular CT complexation, leading to a folded conformation, occurs in small proportions in solutions at ambient temperature and is more favored in less-polar dichloromethane than in acetonitrile. In sharp contrast, the antiparallel dimer CT complex, rather than the folded monomer, is much more favored in dichloromethane at low temperatures, as confirmed by the concentration dependency of the absorption changes and the DFT calculations. In the dimer CT complex, bearing a pair of donor−acceptor interactions, the electronic coupling element, which reflects larger electronic interactions between donor and acceptor, is doubled compared with that of the monomer CT complex. Most interestingly, the circular dichroism spectral behavior of these two complexation modes has been examined to reveal that the *g* factor, especially in the CT transition, is extraordinarily enhanced in the dimeric form, as a result of the more strict fixation of the chiral moiety by the stronger CT interactions.

In the experiments to elucidate the effects of confinement on the structure and chiroptical properties of the CT-dyad, CD and CB were chosen as hosts of different natures, as they can offer completely different environments for inducing discrete guest structures. It was shown that both the naphthalene moiety

and the alkoxyl group of the dyad are shallowly included in the β-CD cavity to afford a much-enhanced *g* factor at the CT transition, probably a result of the fixation of the chiral group upon host−guest interactions and partially a result of the chiral environment of the CDs. Such effects turned out to significantly depend on the size and shape of the CD cavity. While γ-CD also enhances the *g* factor to a lesser extent than β-CD, α-CD and permethylated β- and γ-CD complexes afford much smaller circular dichroism at the ^1L_b band and no detectable Cotton effect at the CT band. In contrast, the dyad is folded into the CB[8] cavity to form a strong intramolecular CT complex, greatly affecting the circular dichroism of the CT transition. Despite the relatively free chiral alkoxy group located outside the CB-[8] cavity, the stronger donor−acceptor interaction enhances the *g* factor of the CT band. Thus, the *g* factor of CT-dyad **1** can be manipulated by choosing the cavity size, shape, and flexibility from almost zero (for the α-CD or the permethylated β- or γ-CD complex) to moderate enhancement (5 ∼ 10 times, for the CB[8] or β-CD complex) and then to significant enhancement (30 times, for the dimer complex formed at low temperatures), which is useful in designing the target compounds for absolute asymmetric synthesis. The following observations are attained from our first quantitative study of the chiroptical properties of the CT-dyad system under confinement and at different temperatures:

(1) The strength and the shape of the Cotton effect on the CT band will be indeed affected by the conformation of the complex. This seems trivial but has not been disclosed so far in how and in what extent. Our experiments gave such quantitative information for the first time.

(2) This allows us to discuss the effect of the size and shape of the confinement more clearly and quantitatively. Indeed, the fixation of the donor part (chiral trigger) alone is found to increase the *g* factor slightly (∼5 times), but the fixation of the whole CT complex in the back-folded manner (in CB[8] cavity) greatly enhances the *g* factor (to a factor of 10).

(3) Enhancement of the *g* factor by dimer formation (CH_2Cl_2, −95 °C) to a factor of 33 is remarkably large. Such an extremely large enhancement was not obtained via any confinement with chiral CDs or achiral CB[8].

(4) The appearance of the new Cotton effect at a longer wavelength, as a result of the forbidden HOMO → LUMO transition, which was originally diminished.

Thus, we have demonstrated that the circular dichroism of the CT band is quite sensitive to the environment (as summarized in Table 4), which would be potentially useful for gathering conformational and stereochemical information in the solution phase by combining this with conventional techniques such as UV−vis, fluorescence, and NMR spectroscopies.

Experimental Section

UV−Vis and Circular Dichroism Spectroscopies. Circular dichroism spectra were measured in a conventional quartz cell (light path, 1 cm) fitted with a temperature controller under the conditions as follows: bandwidth, 1 nm; scan rate, 50 nm/min; response, 8 s; accumulation, 4 times; data interval, 0.1 nm, unless otherwise stated. All of the UV−vis spectra were obtained with the following conditions: bandwidth, 1 nm; scan rate, 100 nm/min; response, medium.

Preparation of *N*-(((*S*)-1-Methylpropyloxy)-2-naphthoxypropyl) 4-Cyanopyridinium Tetrafluoroborate. The crude bromide (0.92 g, 2.0 mmol) was dissolved in MeCN (30 mL) and stirred under an argon atmosphere, while ammonium tetrafluoroborate (4.2 g, 40 mmol, 20 eq), dissolved in H_2O (50 mL), was added all at once. The resulting solution was refluxed for 20 h. The resultant solution was evaporated, filtrated, and washed with water. The crude orange material was reprecipitated twice from acetonitrile/diethyl ether, affording a pale yellow solid material. This salt was dissolved again in MeCN (30 mL), and ammonium tetrafluoroborate (2.4 g, 20 mmol, 10 eq), dissolved in H_2O (50 mL), was added all at once. The resulting solution was refluxed for 18 h. The resultant solution was concentrated and filtrated. The crude orange salt was washed with water and dried under reduced pressure.

***N*-(((*S*)-1-Methylpropyloxy)-2-naphthoxypropyl) 4-Cyanopyridinium Tetrafluoroborate 1.** Yield: 0.99 g, 25% (calculated as 0.5 hydrate). Mp: 125−126 °C (dec; acetonitrile/diethyl ether). MS (FAB, positive mode): m/z = 448 and 361 (M^+ and *N*-(((*S*)-1-methylpropyloxy)-2-naphthoxypropyl) 4-cyanopyridinium). MS (FAB, negative mode): m/z = 87 (BF_4^-). HRMS (FAB): calcd for $C_{23}H_{25}BF_4N_2O_2$, 448.1945; found, 448.1961. ^{1}H NMR (CD_3CN): δ 0.99 (3H, t, J = 7.3 Hz), 1.31 (3H, d, J = 6.2 Hz), 1.65 (1H, pseudo sept d, J = 7.6, 1.2 Hz), 1.75 (1H, pseudo sept d, J = 7.6, 1.2 Hz), 2.52 (2H, br quint, J = 5.9 Hz), 4.18 (2H, t, J = 5.7 Hz), 4.46 (2H, sext, J = 5.9 Hz), 4.85 (2H, t, J = 6.8 Hz), 6.91 (1H, dd, J = 9.2, 2.6 Hz), 7.11 (1H, dd, J = 8.8, 2.6 Hz), 7.13 (1H, d, J = 2.6 Hz), 7.21 (1H, d, J = 2.6 Hz), 7.66 (2H, dd, J = 8.8, 2.2 Hz), 8.34 (2H, br d, J = 6.6 Hz), 8.96 (2H, d, J = 6.6 Hz). ^{13}C NMR (CD_3CN): δ 10.0, 19.5, 29.9, 31.0, 62.1 (br), 65.5, 75.9, 108.1, 109.8, 115.0, 119.5, 121.1, 129.2, 129.5, 130.5, 131.2, 147.4 (t, J = 8.3 Hz), 155.4, 155.8. Specific rotation: $[\alpha]^{25}_D$ +14.6 ± 2.7° (*c* 0.10, CH_2Cl_2). EA (%) calcd for $C_{23}H_{25}BF_4N_2O_2 \cdot 0.5H_2O$: C, 60.41; H, 5.73; B, 2.36; F, 16.62; N, 6.13; O, 8.75. Found: C, 60.34; H, 5.51; N, 6.20.

Acknowledgment. T.M. thanks Alexander von Humboldt-Stiftung for the fellowship. Financial support of this work by a Grant-in-Aid for Scientific Research from the Ministry of Education, Culture, Sports, Science, and Technology of Japan (No. 16750034 to T.M.) and by the Creative Research Initiative Program and International Joint R&D Projects from the Ministry of Science and Technology of Korea (to K.K.) are gratefully acknowledged. We also thank Dr. Guy A. Hembury for assistance in the preparation of this manuscript.

Supporting Information Available: General experimental details, details of absorption, fluorescence, circular dichroism, and 2D NMR spectra of the complexed and uncomplexed **1**, **2**, 2,6-dimethoxynaphthalene, and *N*-methyl-4-cyanopyridinium tetrafluoroborate under a variety of conditions; geometries of optimized conformations of monomeric and dimeric **1** by DFT calculation; and complete ref 5b. This material is available free of charge via the Internet at http://pubs.acs.org.

JO0602672